Recent Progress in Electrocatalytic Reduction of CO$_2$

Chaojun Ren [1] , Wei Ni [1] and Hongda Li [2,*]

1   Beijing Aerospace Propulsion Institute, No.1 South Dahongmen Road, Beijing 100076, China
2   Liuzhou Key Laboratory for New Energy Vehicle Power Lithium Battery, School of Electronic Engineering,
     Guangxi University of Science and Technology, Liuzhou 545006, China
*   Correspondence: hdli@gxust.edu.cn; Tel.: +86-152-0144-0207

Abstract: A stable life support system in the spacecraft can greatly promote long-duration, far-distance, and multicrew manned space flight. Therefore, controlling the concentration of CO$_2$ in the spacecraft is the main task in the regeneration system. The electrocatalytic CO$_2$ reduction can effectively treat the CO$_2$ generated by human metabolism. This technology has potential application value and good development prospect in the utilization of CO$_2$ in the space station. In this paper, recent research progress for the electrocatalytic reduction of CO$_2$ was reviewed. Although numerous promising accomplishments have been achieved in this field, substantial advances in electrocatalyst, electrolyte, and reactor design are yet needed for CO$_2$ utilization via an electrochemical conversion route. Here, we summarize the related works in the fields to address the challenge technology that can help to promote the electrocatalytic CO$_2$ reduction. Finally, we present the prospective opinions in the areas of the electrocatalytic CO$_2$ reduction, especially for the space station and spacecraft life support system.

Keywords: carbon dioxide; electrocatalytic reduction; electrocatalyst; electrolyte; reactor design; spacecraft life support system

1. Introduction

With the continuous development of human science and technology, space exploration will face unprecedented opportunities and challenges [1–5]. Currently, realizing the recycle of materials in closed space stations is the best solution to solve the problem of water (H$_2$O) and oxygen (O$_2$) resupply faced by human activities, which not only can extend the duration of manned missions and reduce transportation costs, but also is a prerequisite for interstellar migration [6–10]. As the end product of human respiration and metabolic processes, carbon dioxide (CO$_2$) carries a large amount of oxygen [11–13]. Therefore, recovering O$_2$ from waste CO$_2$ is an important way to achieve resource recycling and reduce transportation costs for medium- and long-term manned extraterrestrial missions [14–18].

The concentration of CO$_2$ in the space station directly affects the life and health system of the astronauts [19]. To reduce the concentration of CO$_2$ (<0.5%) and maintain the balance of air components, it is necessary to treat the CO$_2$ emissions at 0.7–1.0 kg per person per day. How to better transform and recycle CO$_2$ in the space station has become the focus of researchers [20–23]. The methods of CO$_2$ transformation can be classified into two categories: physical absorption and chemical conversion [24,25]. The chemical conversion mainly includes thermochemistry, photocatalytic reduction, electrocatalytic reduction, and photoelectrocatalytic reduction [26–29]. Chemical conversion can capture and immobilize CO$_2$ or convert it into useful low-carbon fuels, such as CO, CH$_4$, HCOOH, CH$_3$OH, etc. [30–34].

In order to satisfy the requirements of future manned space missions, the development of a new generation of CO$_2$ conversion and oxygen production technologies has become the focus of current space technology research and development [35–39]. Currently, the CO$_2$ reduction techniques used in space stations include Sabatier, Bosch, CO$_2$ electrolysis,

CO$_2$ pyrolysis, and other reduction methods [40–44]. However, the direct conversion of CO$_2$ to small organic molecules is more attractive, and this method can yield more valuable products [45–47]. Among the numerous CO$_2$ conversion methods, electrochemical reduction of CO$_2$ has the advantages of atmospheric temperature, normal pressure, low energy consumption, and minimal environmental pollution [48–51]. Besides, the electrochemical reduction of CO$_2$ can effectively overcome the higher redox potential of reaction intermediates, which has better application prospects and significance [52–54]. However, the electrochemical conversion of CO$_2$ still faces many challenges, and it needs to satisfy two basic criteria, i.e., high energy efficiency and high reaction rate [55–59].

Here, we summarize the related works in the fields to address the challenge technology that could help to promote the electrocatalytic CO$_2$ reduction. Finally, we present the prospective opinions in the areas of the electrocatalytic CO$_2$ reduction, especially for the space station and spacecraft life support system.

2. The Mechanism of Electrocatalytic Reduction of CO$_2$

The electrocatalytic reduction of CO$_2$ often occurs at the interface between the electrode and the electrolyte, and the electrolyte is usually an aqueous solution of potassium bicarbonate [19]. As shown in Figure 1, the multiphase catalytic process generally consists of four main steps: (i) The CO$_2$ in the solution diffuses to the surface of the working electrode. (ii) The electrocatalyst adsorbs CO$_2$ from the solution. (iii) Electron transfer or proton migration is used to cleave C-O bonds or form C-H bonds. (iv) The generated products are detached from the electrocatalyst surface and diffused into the electrolyte [60,61]. The adsorption of CO$_2$ on the electrocatalyst surface is an important step in the whole reaction. During the adsorption process, the C=O bonding is strongly perturbed by the substrate, and the electrons are shared between the CO$_2$ and the catalyst. A number of reaction mechanisms have been proposed for the conversion of CO$_2$. It is widely accepted that the reactive species are the neutral hydrated CO$_2$ molecules, and they will convert into CO$_2^{\bullet-}$ in the adsorption process on most of the main-group metal electrodes in aqueous media. Then the absorbed CO$_2^{\bullet-}$ reacts with the H$_2$O molecules to form HCO$_2^{\bullet}$. The intermediate would convert into to HCO$_2^-$ because of its unstable unpaired electron, followed by the desorption of HCO$_2^-$ species [60].
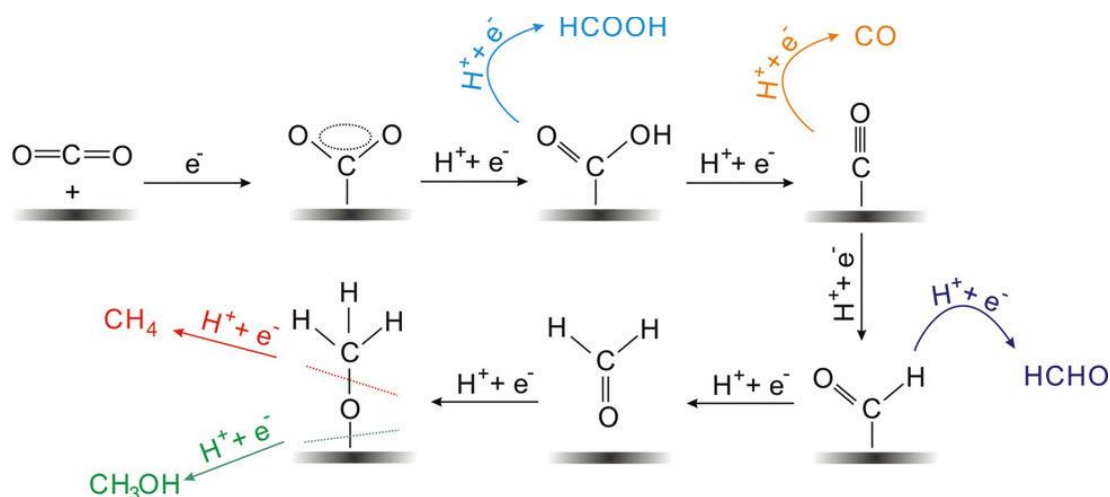

Figure 1. Reaction mechanism of electrochemical CO$_2$ reduction on electrodes in aqueous solutions and the formation paths for the five main C1 products during the reduction process. Reprinted from Ref. [60], copyright (2017), with permission from Wiley.

Because of the complexity of electrocatalysis, this leads to the fact that the chosen electrocatalyst and the applied electrode potential have a strong influence on the final reduction product [62]. In general, the reaction products are carbon compounds with

different oxidation states [63,64]. The electrocatalytic reduction mechanism of CO_2 is a complicated process that involves multiple electron transfer reactions, typically including 2-, 4-, 6-, or 8-electron reaction pathways [65,66]. Table 1 summarizes the corresponding standard reduction potentials for the C1 products (C, CO, HCOOH, CH_2O, CH_3OH, and CH_4) and C2 products (C, CO, HCOOH, CH_2O, CH_3OH, and CH_4) obtained by electrocatalytic reduction of CO_2. Overall, the required potential to generate C=O products (except $H_2C_2O_4$) is greater than that of generating compounds containing C–H and C–OH.

Table 1. The standard potential for the conversion of CO_2 to various C1 and C2 products in aqueous solution under standard conditions (1.0 atm and 25 °C). Reprinted from Ref. [45], copyright (2014), with permission from the Royal Society of Chemistry.

Half Electrochemical Thermodynamic Reactions	Standard Potentials (V vs. SHE)
CO_2 (g) + $2H^+$ + $2e^-$ = HCOOH (l)	−0.250
CO_2 (g) + $2H_2O$ (l) + $2e^-$ = $HCOO^-$ (aq) + OH^-	−1.078
CO_2 (g) + $2H^+$ + $2e^-$ = CO (g) + H_2O (l)	−0.106
CO_2 (g) + $2H_2O$ (l) + $2e^-$ = CO (g) + $2OH^-$	−0.934
$2CO_2$ (g) + $2H^+$ + $2e^-$ = $H_2C_2O_4$ (aq)	−0.500
$2CO_2$ (g) + $2e^-$ = $C_2O_4^{2-}$ (aq)	−0.590
CO_2 (g) + $4H^+$ + $4e^-$ = C (s) + $2H_2O$ (l)	0.210
CO_2 (g) + $2H_2O$ (l) + $4e^-$ = C (s) + $4OH^-$	−0.627
CO_2 (g) + $4H^+$ + $4e^-$ = CH_2O (l) + H_2O (l)	−0.070
CO_2 (g) + $3H_2O$ (l) + $4e^-$ = CH_2O (l) + $4OH^-$	−0.898
CO_2 (g) + $6H^+$ + $6e^-$ = CH_3OH (l) + H_2O (l)	0.016
CO_2 (g) + $5H_2O$ (l) + $6e^-$ = CH_3OH (l) + $6OH^-$	−0.812
CO_2 (g) + $8H^+$ + $8e^-$ = CH_4 (g) + $2H_2O$ (l)	0.169
CO_2 (g) + $6H_2O$ (l) + $8e^-$ = CH_4 (g) + $8OH^-$	−0.659
$2CO_2$ (g) + $12H^+$ + $12e^-$ = CH_2CH_2 (g) + $4H_2O$ (l)	0.064
$2CO_2$ (g) + $8H_2O$ (l) + $12e^-$ = CH_2CH_2 (g) + $12OH^-$	−0.764
$2CO_2$ (g) + $12H^+$ + $12e^-$ = CH_3CH_2OH (l) + $3H_2O$ (l)	0.084
$2CO_2$ (g) + $9H_2O$ (l) + $12e^-$ = CH_3CH_2OH (l) + $12OH^-$	−0.744

Thermodynamically, the equilibrium potential of CO_2 reduction is comparable to the equilibrium potential of hydrogen evolution reaction (HER) [67,68]. This means that the electrocatalytic reduction of CO_2 is accompanied by severe HER, which leads to a decrease in the efficiency of the CO_2 reduction. In addition, the CO_2 reduction products possess small thermodynamic potential difference, indicating that it is difficult to reduce CO_2 to specific products with good selectivity and conversion efficiency in the current CO_2 reaction [69,70]. Driving the CO_2 reduction reaction often requires a larger overpotential, which further contributes to the technical difficulty of electrocatalytic CO_2 reduction [45]. Therefore, the development of efficient electrochemical CO_2 reduction capable of promoting multielectron (and proton) transfer is a major task in this field.

3. Electrocatalysts

Over the past few decades, researchers have attempted to develop high-performance CO_2 electrocatalysts and have carried out extensive work [71–73]. The catalysts could reduce the activation energy required for the electroreduction of CO_2, thereby minishing the reduction overpotential and current density. Most of the studies have focused on transition-metal-based catalysts, which are mainly Cu, Au, Fe, Ag, Re, Mn, Co, Ni, Pd, Ir, Ru, etc. [17,74–76]. The main forms of the complexes include transition metal polypyridines, metal porphyrins/phthalocyanines, and various metal phosphine complexes [77,78]. It was found that transition metal complexes were used for the electrocatalytic reduction of CO_2 and presented outstanding performance. Some reported electrocatalysts for electrocatalytic CO_2 reduction are summarized in Table 2 and are illustrated in detail in the following sections.

Table 2. Summary of the performance of typical electrocatalysts for electrocatalytic CO_2 reduction.

Electrocatalyst	Potential (V vs. RHE)	Major Products	FE (%)	Reference
Cu–In alloys (In: 80 at%)	−1.0	formate	62.0	2017 [79]
CuS@Ni Foam	−1.1	methane	73.0	2017 [80]
$Co(CO_3)_{0.5}(OH)\cdot0.11H_2O$	−0.98	methane	97.0	2018 [81]
Co/Zn@ZIFs	−0.52	CO	94.0	2018 [82]
ultrathin Pd nanosheets	−0.5	CO	94.0	2018 [83]
Mn−doped In_2S_3	−0.9	formate	86.0	2019 [84]
Ni_1–N_2–C	−0.8	CO	96.8	2019 [85]
Ni/Fe–N–C–DAC	−0.7	CO	99.0	2019 [86]
Pd–Au	−0.5	CO	80.0	2019 [87]
ultrathin porous Cu nanosheets	−1.0	CO	74.1	2019 [88]
Cu nanocubes	−0.5	C_2H_4	60.0	2019 [89]
Fe–N_5–C	−0.46	CO	97.0	2019 [90]
Fe–N_4–C	−0.5	CO	94.9	2019 [91]
Fe^{3+}–N–C	−0.45	CO	90.0	2019 [92]
Ni−graphene oxide	−0.63	CO	96.5	2019 [93]
Ni−N_4−C	−0.65	CO	90.0	2019 [94]
Ni−N_2−C	−0.8	CO	98.0	2019 [95]
InN NSs	−0.9	formate	91.0	2020 [96]
NiSn−APC	−0.82	formate	86.1	2020 [97]
Ni_{20}−N−C	−0.53	CO	97	2020 [98]
Cu−Al	−1.50	C_2H_4	80	2020 [99]
5 nm In_2O_3 NPs	−0.7	formate	80.0	2021 [100]
Pb_1Cu	−0.8	formate	96.0	2021 [101]
SAC−Ag/g−C_3N_4	−0.7	CO	93.7	2021 [102]
40Ni@N−C/rGO	−0.97	CO	92.0	2021 [103]
polycrystalline SnS_x NFs	−1.0	formate	97.0	2022 [104]
In_2O_3@In−Co PBA	−0.96	formate	85.0	2022 [105]
Sb−SAs/NC	−0.8	formate	94.0	2022 [106]
Nb−N−C	−0.8	CO	90.0	2022 [107]

Among the transition metal complexes, Cu complexes had better activity. Recently, Raja et al. [78] designed a dinuclear Cu (I) complex as catalysts for the electroreduction of CO_2, and its catalytic cycle is shown in Figure 2 below. They found that the Cu (I) system could be oxidized by CO_2, which suggested that the selective bonding of CO_2 and Cu (I) ions could provide a low-energy pathway for the formation of $CO_2^{\bullet-}$ radical anions. Thus, the Cu (II) tetranuclear oxalate-bridged complex $[2]^{4+}$ was thermodynamically favorable. Moreover, the bonding of CO_2 to the Cu(I) center in the dinuclear copper (I) complex $[1]^{2+}$ was faster and has a higher selectivity. This was due to the low solubility of lithium oxalate in acetonitrile, and the release of the oxalate double anion from $[2]^{4+}$ in the presence of $LiClO_4$ could be accomplished instantaneously, and the dinuclear copper (II) complex $[4]^{4+}$ was produced. Consequently, the electrocatalytic reduction of Cu (II) ions to Cu (I) might be the rate-controlling step in this system. The electrode surface was coated by the lithium oxalate generated during the reaction and then prevented the effective electron transfer.

Cu electrodes have good catalytic performance for the conversion of CO_2 to alkanes and alcohols [64]. The moderate hydrogen evolution overpotential of Cu electrodes can properly suppress the hydrogen production. Therefore, Cu electrodes can generate relatively high current efficiency [108]. Recently, Matthew et al. [109] prepared Cu-modified electrodes by calcining Cu sheets in air and then further electrochemically reducing and calcining the generated Cu_2O (Figure 3). The activity exhibited by such electrodes in reducing CO_2 was highly dependent on the initial thickness of the Cu_2O layer. The experimental results showed that the activity of the electrodes prepared from a Cu_2O thin layer at 130 °C was not different from that of polycrystalline Cu. However, the Cu_2O electrode formed by calcination at 500 °C with a thickness of not less than 3 μm had a large roughness coefficient, and its overpotential was 0.5 V smaller than that of polycrystalline Cu in the reduction of CO_2. More significantly, the current density of this electrode would be higher than

1 mA/cm^2 at an overpotential lower than 0.4 V, which was larger than the reported activity of other metal electrodes. Meanwhile, the Cu-modified electrode obtained by calcination at 500 °C remained stable after reacting for 7 h, while the polycrystalline Cu electrode started to passivate within 1 h under the same circumstances.
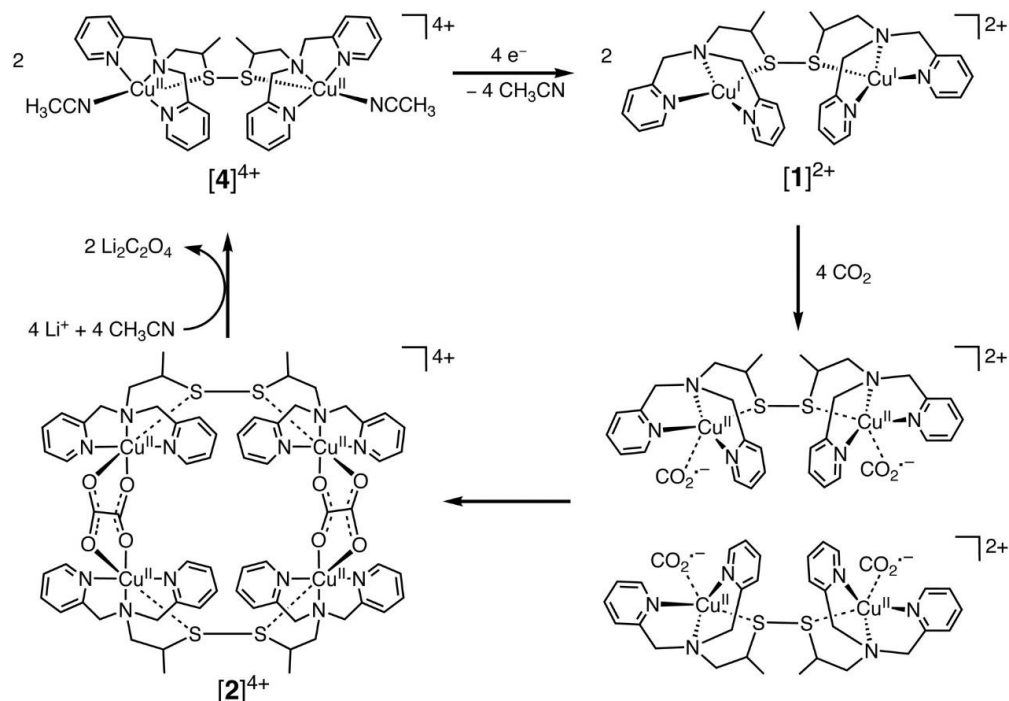

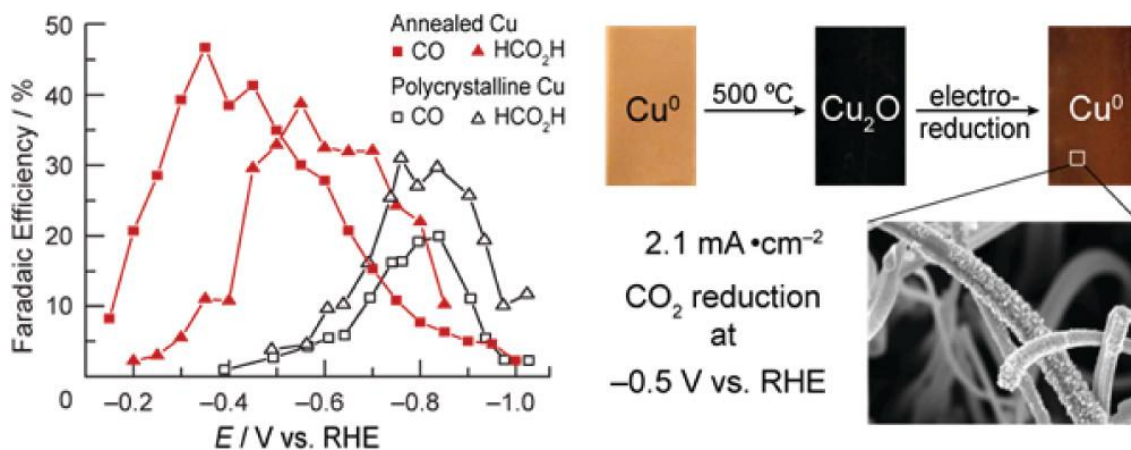**Figure 2.** Proposed electrocatalytic cycle for oxalate formation. Reprinted from Ref. [78], copyright (2010), with permission from the American Association for the Advancement of Science.

Figure 3. Electrocatalytic performance and the preparation process of Cu electrodes. Reprinted from Ref. [109], copyright (2012), with permission from the American Chemical Society.

To confirm that different components of binary nanocrystals have different effects on the performance of the electrocatalytic reduction of CO$_2$, Guo et al. [110] investigated the performance of Cu-Pt binary alloy nanocrystals for the electrochemical reduction of CO$_2$ in 0.5 M KHCO$_3$ at room temperature. As shown in Figure 4, it was found that among Cu-Pt nanocrystals with different molar ratios, the catalyst with a molar ratio of 3:1 had the best activity for the catalytic reduction of CO$_2$, the lowest onset potential (-0.972 V), and the highest current density (0.598 mA/cm^{-2}, -1.3 V vs. SCE). The optimization of catalyst components was compared, and a reasonable mechanism hypothesis was proposed. As illustrated in Figure 5, Pt had a unique adsorption capacity for protons, and it was

an efficient catalyst for HER, leading that H_2O molecules in solution would be adsorbed on Pt atoms in Cu-Pt nanocrystals. CO*, the reaction intermediate generated by CO_2 gaining electrons, was adsorbed on Cu atoms, and then combined with H^+ provided by H_2O to generate HCO* and finally CH_4. The above mechanism well explains why Cu-Pt nanocrystals with a molar ratio of 3:1 had the highest activity in the catalytic reduction of CO_2. In the process of CH_4 generation, CO* and H^+ were indispensable, and Cu promoted CO_2 to gain electrons to generate CO*. Pt facilitated the adsorption of H_2O to generate H^+, so the molar ratio of Cu-Pt had an optimal value; too much Pt or Cu was not conducive to CH_4 production.
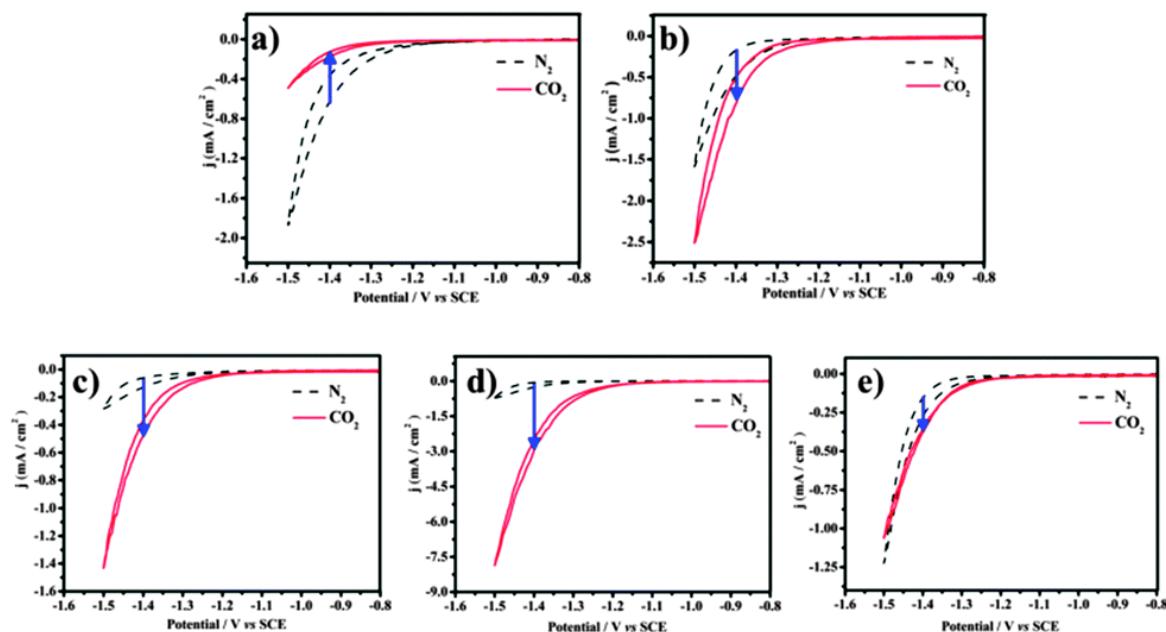

Figure 4. The cyclic voltammograms of catalysts were recorded in N_2- and CO_2-saturated 0.5 M $KHCO_3$ with a scan rate of 10 mV/s^{-1} between -0.8 and -1.5 V (vs. SCE). (**a**) Cu-Pt-1#, (**b**) Cu-Pt-2#, (**c**) Cu-Pt-3#, (**d**) Cu-Pt-4#, and (**e**) Cu-Pt-5#. Reprinted from Ref. [110], copyright (2015), with permission from the Royal Society of Chemistry.
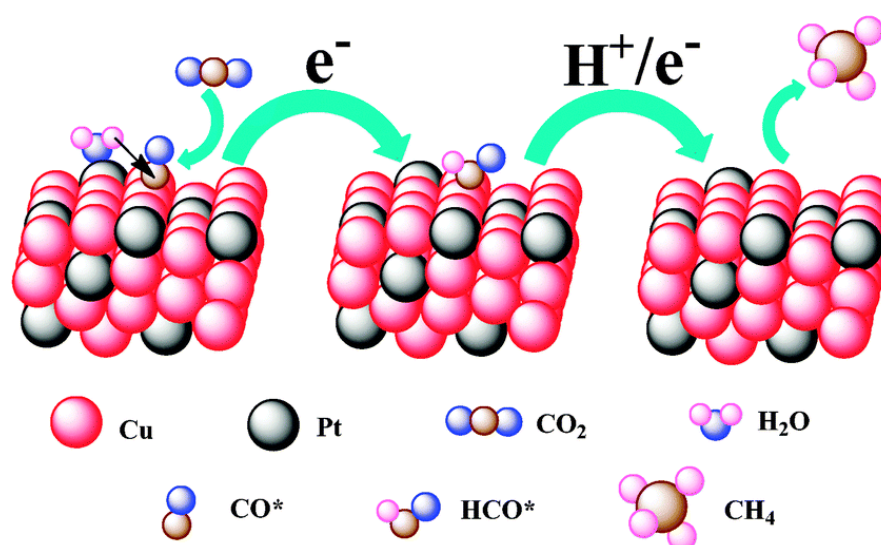

Figure 5. A proposed mechanism illustrating the steps of CO_2 electroreduction and CH_4 formation occurring at the Cu-Pt 3:1 NC catalyst. Reprinted from Ref. [110], copyright (2015), with permission from the Royal Society of Chemistry.

However, Cu-based catalysts still faced some problems because the instability of Cu materials was easily deactivated and decomposed during the catalytic reduction of CO_2. Some prepared Cu-based catalysts were easily oxidized when exposed to air [21,75,109]. The valence and morphology changes of Cu-based catalysts during the catalytic process should be deeply elucidated, which conduced to provide a crucial role. Ni et al. [111] proposed a modulation strategy: hydrogen reduction valence, which could simply regulate the ratio of different valence states of Cu by optimizing the reduction time, and helped to investigate the mechanism of multivalent Cu in depth. The experimental results showed that the excellent performance of G-Cu$_x$O-2h not only stabilized the intermediate product $CO_2^{\bullet-}$, but also accelerated the rate-limiting step in the $HCOO^-$ desorption process, which was related to the optimal Cu (I) content in the catalyst. The paper also proposed a "buffering effect" to explain the stability of G-Cu$_x$O-2h, as shown in Figure 6. Cu (II) from the thicker subsurface layer acted as a sacrificial source to supplement Cu (I), thus balancing the Cu (I) content in the surface layer and maintaining the activity of the catalyst in the reaction.
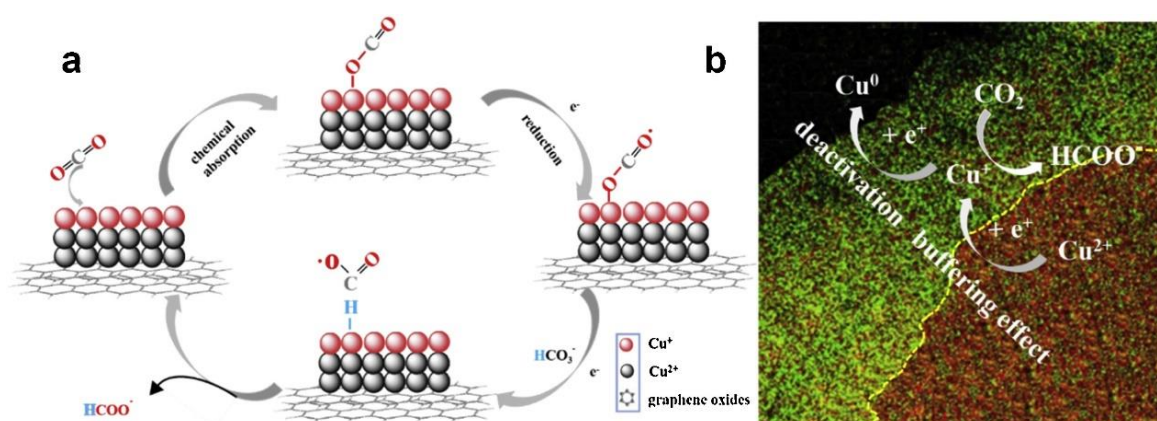

Figure 6. (**a**) A proposed mechanism illustrating the steps of electrochemical CO_2 reduction and the formation of HCOOH occurring at the G-Cu$_x$O-2 h electrocatalyst. (**b**) A proposed "buffering effect" illustrating the origin of the durability of G-Cu$_x$O-T electrocatalysts. Reprinted from Ref. [111], copyright (2019), with permission from Elsevier.

Furthermore, the electrocatalytic reduction of CO_2 at the Au electrode has also been investigated by Matthew et al. [112]. They used the periodically symmetric square wave potential method to prepare an amorphous Au_2O_3 layer on a Au electrode. This electrode was used directly for the electrocatalytic reduction of CO_2, in which Au_2O_3 was reduced to Au within 15 min. The electrode exhibited high selectivity for the product CO in the reduction of CO_2 with an overpotential of only 0.14 V, and the activity was maintained for at least 8 h. The authors attributed the high activity of such catalysts to the increased stability of the $CO_2^{\bullet-}$ intermediate; the electrolyte HCO_3^- acted as H^+ donors during the catalytic process (Figure 7).

Gao et al. synthesized a Pd nanoparticle electrode and efficiently catalyzed the reduction of CO_2 to CO. They found that Pd nanoparticle size exhibited significant size dependence in the range of 2.4–10.3 nm [113]. With the Pb nanoparticle size changes from 10.3 to 3.7 nm, the Faraday conversion efficiency of CO generation at -0.89 V increased from 5.8% to 91.2%, while the current density of CO generation was enhanced 18.4 times (Figure 8). The relationship between catalyst performance and particle size was obtained using the density functional theory (DFT) to further analyze the free energy of CO_2 reduction and HER at three different reaction sites: plane, step, and corner. The results indicated that the relationship between the conversion frequency (TOF) of CO generation and catalyst particle size presented a volcano-like curve (Figure 9). This illustrated that CO_2 adsorption, COOH* formation, and CO* removal could be modulated by changing

the size of Pb nanoparticles, thus enabling the transition of Pd nanoparticles from HER catalysts to efficient CO_2 reduction catalysts.
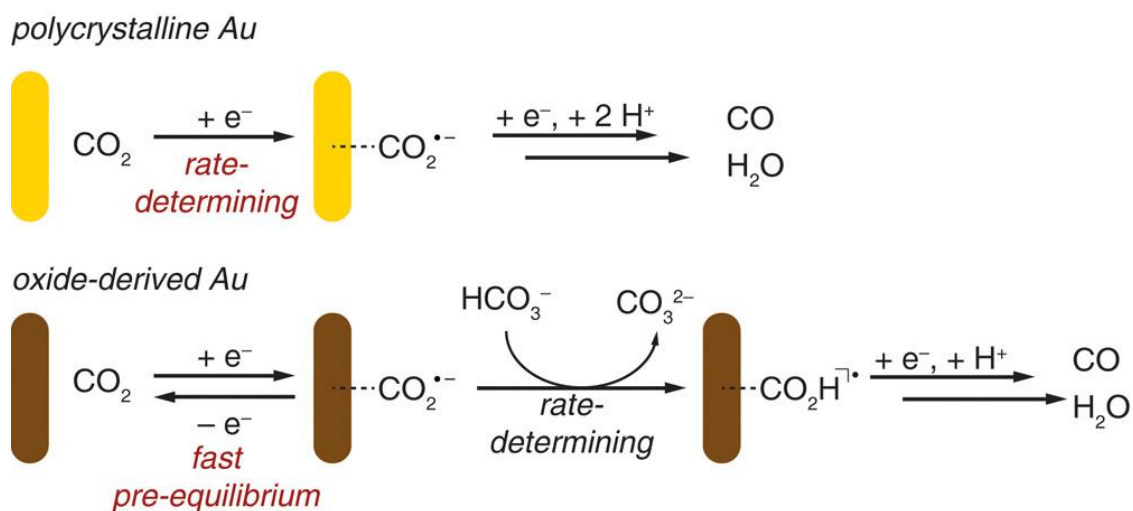

Figure 7. Proposed mechanisms for CO_2 reduction to CO on polycrystalline Au and oxide-derived Au. Reprinted from Ref. [112], copyright (2012), with permission from the American Chemical Society.
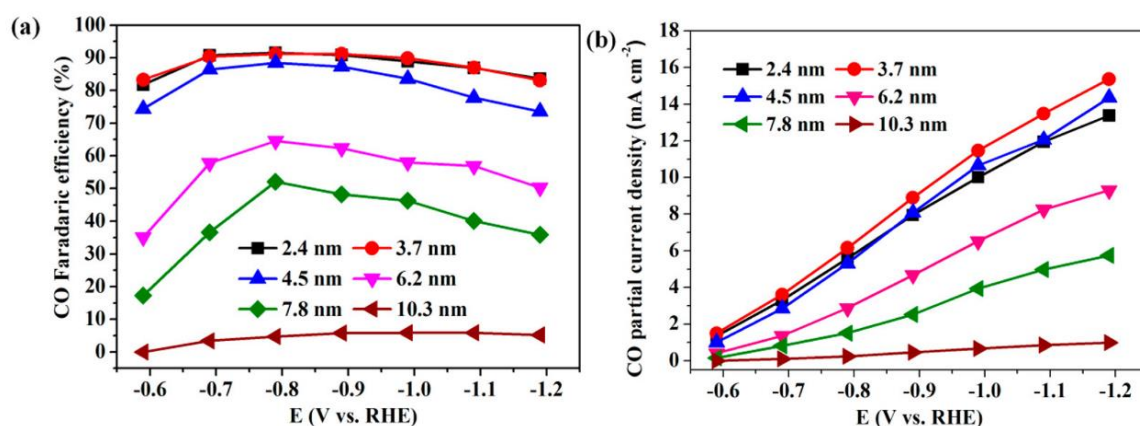

Figure 8. Applied potential dependence of (**a**) Faradaic efficiencies and (**b**) current densities for CO production over Pd NPs with different sizes. Reprinted from Ref. [113], copyright (2015), with permission from the American Chemical Society.

As well known, the metal electrode possessed high activity for the catalytic reduction of CO_2 [114,115]. The outstanding catalytic activity was obtained by reducing metal oxides to metal electrode [116–118]. This electrode could decrease the reduction potential of CO_2 to a thermodynamic minimum. In comparison, other preparation methods caused many microstructural changes in the catalysts, such as interfaces and defects [119–121]. The influence of metal oxides on the catalytic performance of metals was related to these microstructures. However, the mechanism of the above system was not clear [122,123]. Recently, a 4-atomic-layer-thick Co oxidized heterostructure (see Figure 10) was prepared by Gao et al. by means of ligand-confined growth and used to explain the effect of metal surface oxides on their own electroreduction CO_2 properties [124]. This work demonstrated that metal atoms located in specific oxidation states enabled the production of higher catalytic activity through specific arrangements, thus providing a new idea for the development of efficient and stable catalysts for CO_2 reduction. It was important for promoting research on the mechanism of metal oxides' electrocatalytic reduction of CO_2.
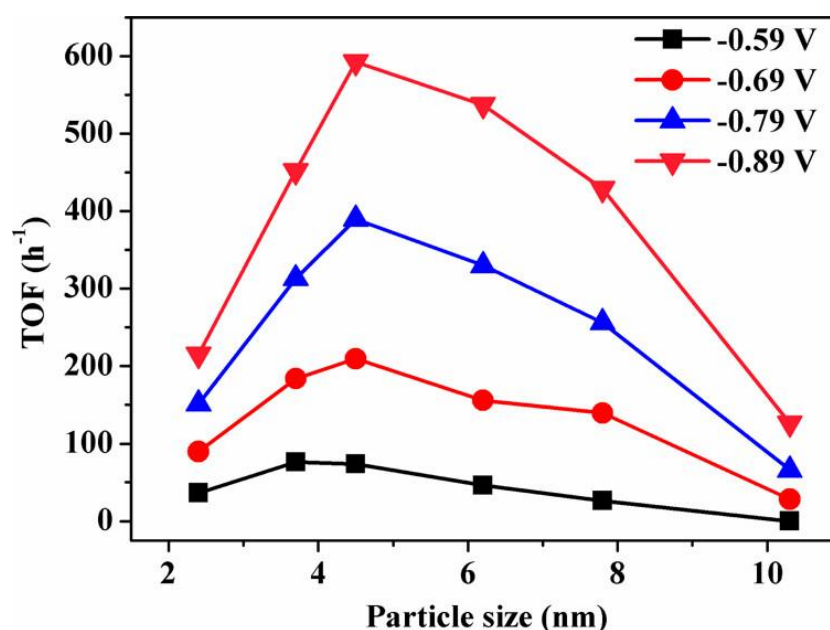
Figure 9. Size dependence of TOF for CO production on Pd NPs at various potentials. Reprinted from Ref. [113], copyright (2015), with permission from the American Chemical Society.
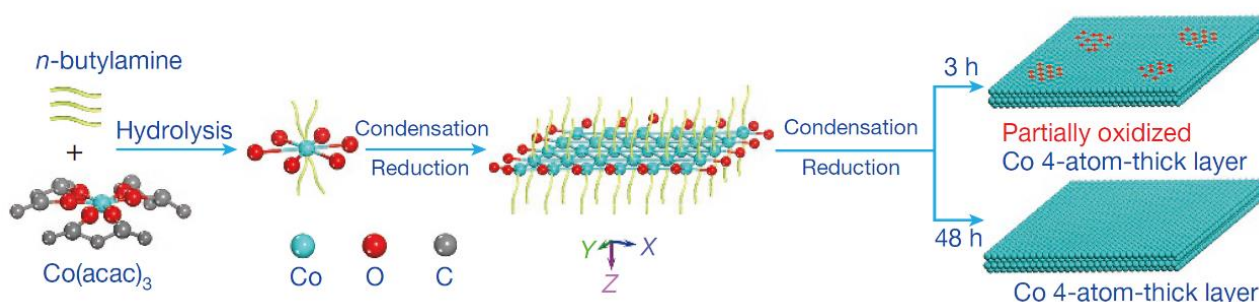

Figure 10. Schematic formation process of the partially oxidized and pure-Co 4-atomic-layer, respectively. Reprinted from Ref. [124], copyright (2016), with permission from Springer Nature.

Transition metal porphyrins have also shown superior reactivity in catalysts for the electrocatalytic reduction of CO_2, such as iron porphyrins and cobalt porphyrins [125]. Cyrille et al. found that the modified iron porphyrins accelerated the reduction reaction of CO_2 after the introduction of phenolic groups in all the neighbors of the iron porphyrin phenyl group. It was concluded that the increased activity of iron porphyrins was related to the high local concentration of protons associated with the phenolic hydroxyl substituents; the relationship between the high turnover frequency (TOF) and the small overpotential (η) of the catalyst was systematically investigated (Figure 11) [77].

Cobalt porphyrins as catalysts for the electrocatalytic reduction of CO_2 have a relatively high overpotential ($-1.3 \sim -1.6$ V vs. SHE) and a low TOF. The possible catalytic mechanism of cobalt porphyrins was analyzed by Kevin et al. using DFT calculations [126]. From the calculations, it was clear that CO_2 was bonded to the particle $[Co(I)P]^-$, and the mechanism is shown in Figure 12. Besides, the presence of water played a crucial role because the key intermediates $[Co(I)P\text{-}CO_2]^{2-}$ and $[Co(II)P\text{-}CO_2H]^-$ were stabilized by hydrogen bonding interaction, which caused the exothermic breakage of the C-O bond. Theoretical calculations also revealed that the electron transfer between the gas diffusion electrode and the polymerized porphyrin catalyst was the rate-controlling step of the whole reaction. These findings were important implications for the capture and the electrochemical reduction of CO_2, respectively.
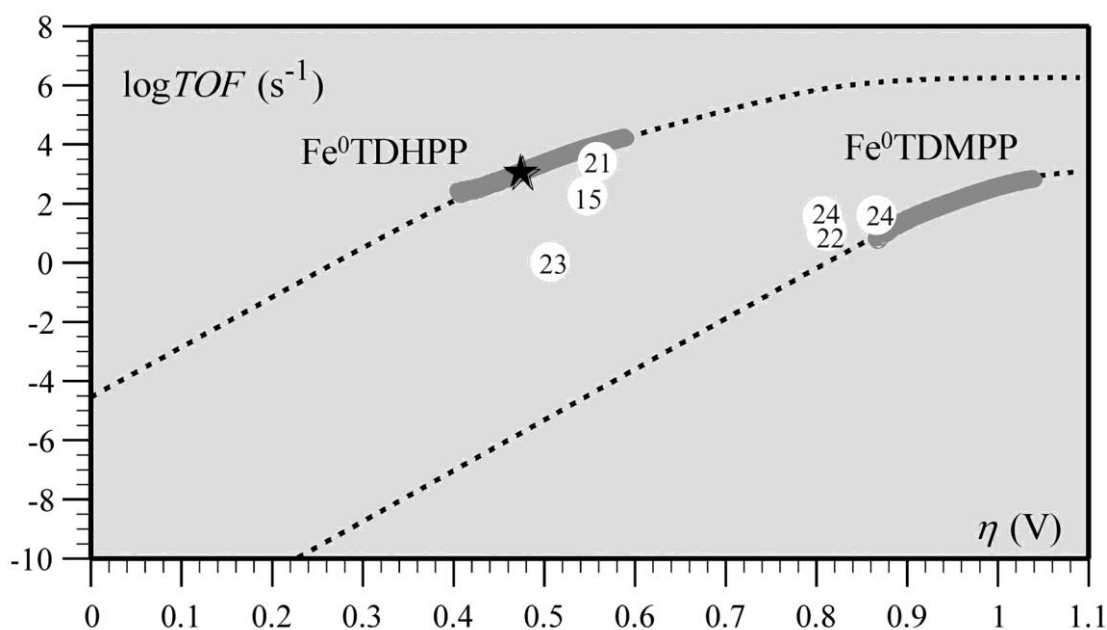
Figure 11. Correlation between turnover frequency and overpotential for the series of CO_2-to-CO electroreduction catalysts. The star indicates TOF and η values from preparative-scale experiments of Fe^0TDHPP. Reprinted from Ref. [77], copyright (2012), with permission from the American Association for the Advancement of Science.
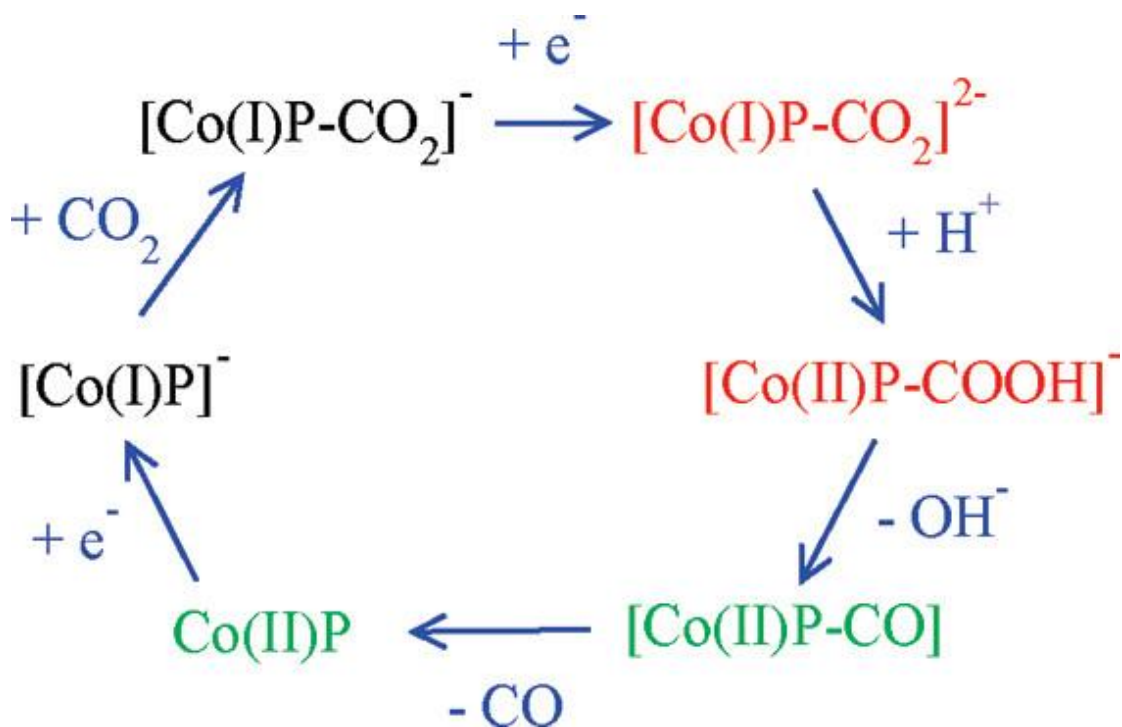

Figure 12. Mechanism of CO_2 reduction with electron addition deduced from hybrid DFT plus dielectric continuum redox potential calculations. Red denotes key intermediates; green species should undergo fast reactions. Reprinted from Ref. [126], copyright (2010), with permission from the American Chemical Society.

The effect of organometallic Ag catalysts supported by carbon–nitrogen in the electrochemical conversion of CO_2 was investigated by Claire et al. [127]. It was shown that such catalysts decreased the reaction overpotential and improved the selectivity, which also

led to an enhanced reaction rate for CO_2 reduction. Moreover, these nitrogen-containing compounds might act as cocatalysts in the electrochemical reduction of CO_2, create a coordinated effect with the Ag surface, and thus facilitate electron transfer. Remarkably, they found that not all nitrogen-containing atoms introduced to the carbon surface exhibited the properties of such catalysts. Therefore, to further enhance the activity and selectivity, a more in-depth study of the CO_2 reduction mechanism was needed to elucidate the interactions between these complexes and the carbon substrate.

Agarwal's group carried out an in-depth study of the CO_2 reduction mechanism. Although the results were based on the photocatalytic reduction of CO_2, their systematic analysis of the CO_2 reduction mechanism was equally applicable in the direction of electrocatalytic reduction of CO_2 [128]. First, they found that tricarbonyl Re complexes, such as Re(bpy)(CO)$_3$Cl (bpy=2,2′-dipyridine), exhibited high activity in catalytic CO_2 reduction in the presence of electron sacrificial agents. Subsequently, they investigated the potential pathway of formate generation by the Re-hydride insertion theory in the presence of triethylamine (TEA) using DFT. It was suggested that TEA was the main donor of hydrogen atoms and electrons, and its catalytic cycle pathway is shown in Figure 13.
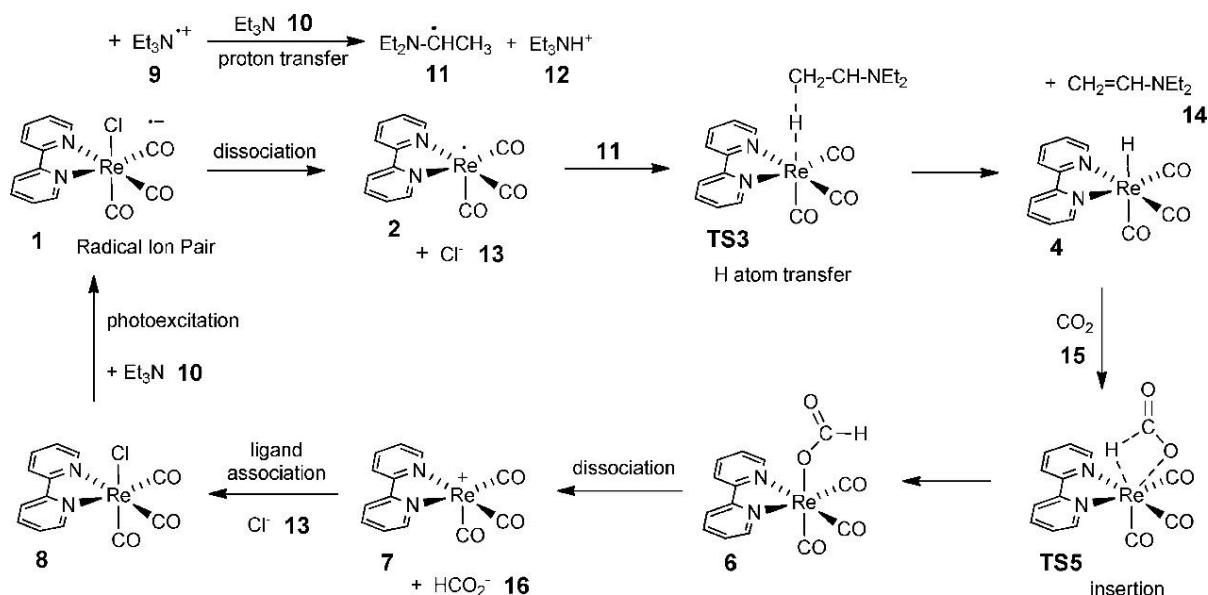

Figure 13. Computed photocatalytic cycle for CO_2 reduction on a Re catalyst. Reprinted from Ref. [128], copyright (2011), with permission from the American Chemical Society.

4. Electrolyte

The influence of the composition of the electrolyte on the CO_2 reduction cannot be ignored [129,130]. Therefore, the study of electrolyte is of great importance to optimize the conditions for the electrochemical reduction of CO_2. Researchers have conducted numerous studies on the electrolyte used for the electrocatalytic reduction of CO_2 [131–133]. Agoritsa et al. found that the rate of electrochemical reduction CO_2 increased in the order of electrolyte cations: $Na^+ < Mg^{2+} < Ca^{2+} < Ba^{2+} < Al^{3+} < Zr^{4+} < Nd^{3+} < La^{3+}$, where the rate of La^{3+} was twice as high as that of Na^+ at the same potential [134]. The increasing order of halogen anions was $Cl^- < Br^- < I^-$. In addition, the conclusions reached by different researchers about the effect of electrolyte ions often differed or even conflicted with each other, which may be due to the fact that researchers only discussed the effect of certain factors on the reaction process and neglected other factors, such as the operation time, the conductivity of the solution, the solubility of CO_2, the concentration of the product at the cathode, and some hydrodynamic factors and their interactions [135].

Moreover, the electrolyte synergistically promoted electrode catalytic reactions to accelerate the electrochemical reduction of CO_2 [136–140]. Kotaro et al. investigated the

effect of Cu wire electrodes in 3 mol L^{-1} of KCl, KBr, and KI electrolytes with X^- (Cl^-, Br^-, I^-) on the electrocatalytic reduction process of CO_2 [141]. It was shown that Cu-X acted as a catalytic layer, facilitating the transfer of electrons from the electrode to CO_2. The electron transfer to CO_2 might be accomplished by X–C bonding, and the X–C bonding was formed by electron flow between the specific adsorbed halogen anion and the empty orbital of CO_2 (Figure 14). The stronger the adsorption of the halogen anion on the electrode, the more CO_2 was bound, which in turn generated a higher CO_2 reduction current. The specific adsorbed halogen anion could also inhibit the adsorption of protons, which in turn generated a higher hydrogen overpotential. This interaction and influence minished the CO_2 reduction overpotential while allowing the rate of electrochemical CO_2 reduction to be enhanced.
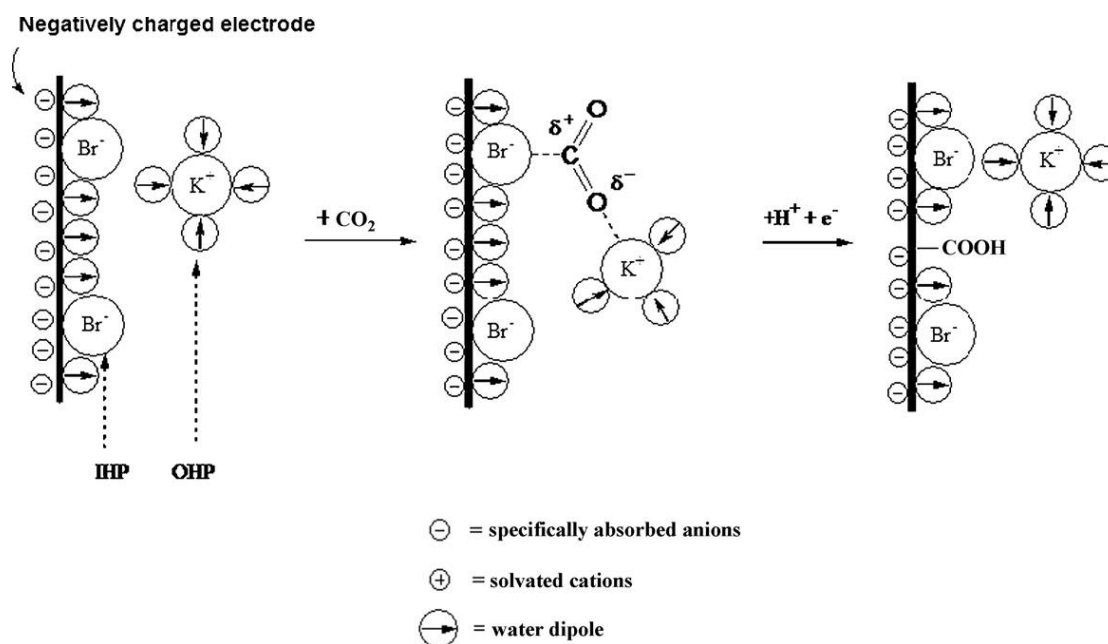

Figure 14. Schematic of specifically adsorbed anions (Br^-), approach of CO_2, and subsequent electrochemical reduction. Reprinted from Ref. [141], copyright (2010), with permission from Elsevier.

Nonaqueous organic solvents can also be used as electrolytes for the electrochemical reduction of CO_2 (such as CH_3CN) [142–144]. Electrocatalytic reduction of CO_2 in organic solvents has the following advantages over water: (1) the solubility of CO_2 is greater than in water; (2) competitive reactions for CO_2 reduction (H_2 generation) can be suppressed; (3) it is used as a potent and better CO_2 absorber for industrial applications, and the process is more energy efficient; and (4) the possibility of reduction below 0 °C is realized. Electrolytes are currently studied in several directions: methanol, ionic liquids, acetonitrile–ionic liquid mixtures, iodomethane–ionic liquid mixtures, and methanol–potassium–ionic liquid mixtures [145].

5. Reactor Design

The structural design of the reactor and the transport of the material have a greater influence on the CO_2 reduction [146,147]. In recent years, several articles have reported several reactor designs, most of which were based on fuel cell designs and used polymer electrolyte membranes to separate the anode from the cathode. Subramania used a composite perfluoropolymer cation exchange membrane (Nafion) to separate the anode from the cathode and to perform the CO_2 reduction reaction at room temperature [148]. This continuous reactor was a great improvement over the intermittent reactor. The maximum current efficiency of formate formation reached 93%; the concentration of formate was up to 0.015 mol L^{-1}.

The alkaline polymer electrolyte membrane cell for the electrochemical conversion of CO_2 was further investigated by Narayanan et al. [149]. The specific structure of this cell is shown in Figure 15. The advantages of this type of reactor were that (1) the reduction products of CO_2 could be saved from reoxidation by the O_2 electrode, (2) a nonprecious metal and its oxide could be used as catalysts, (3) the integrated compact porous electrode structure achieved a low internal resistance of the cell, and (4) it was scaled up to large sizes with no efficiency loss.
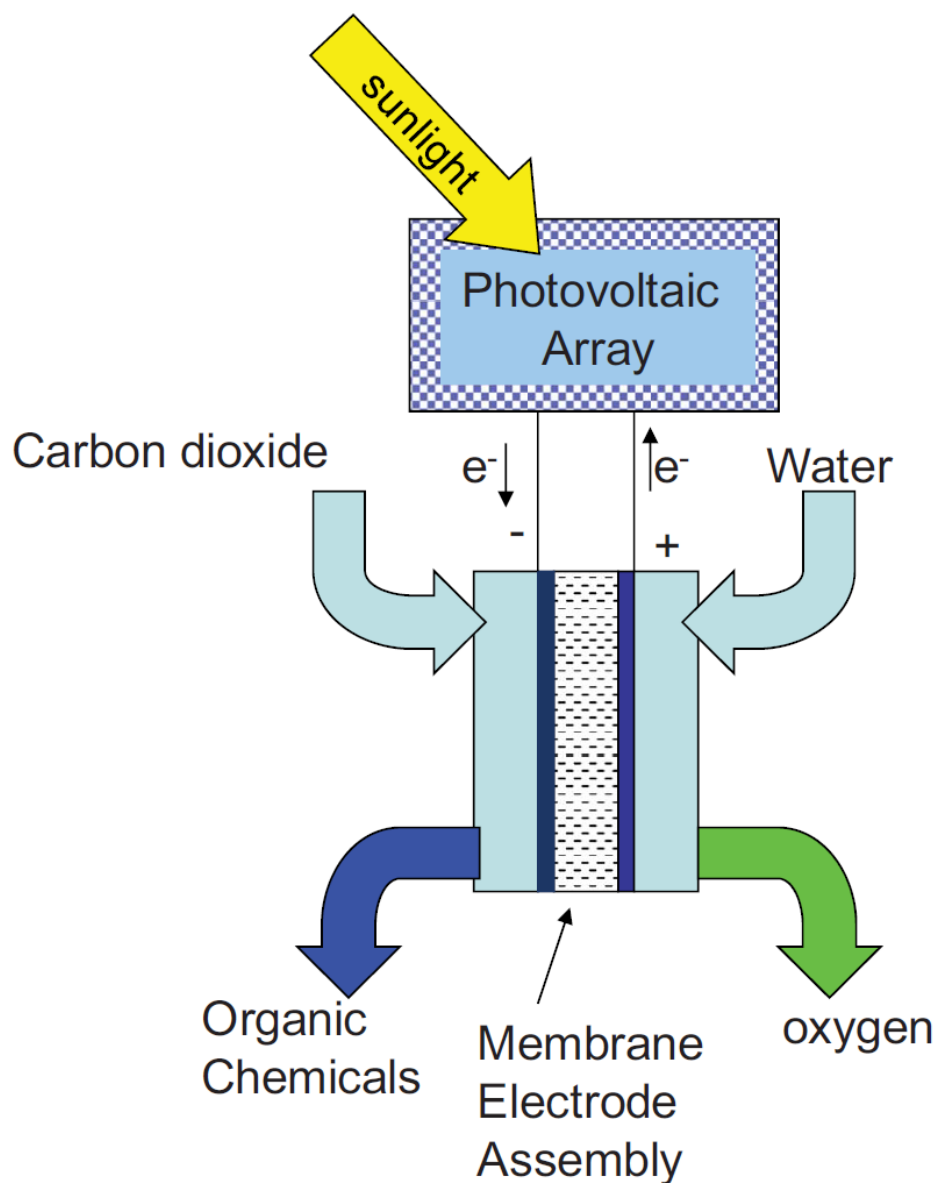

Figure 15. Polymer membrane cell configuration for the electrochemical reduction of carbon dioxide. Reprinted from Ref. [149], copyright (2010), with permission from the Electrochemical Society.

Besides, Claudio et al. designed a novel photoelectrocatalytic (PEC) reactor for the synthesis of solar fuels [150]. The internal configuration of this device is depicted in detail in Figure 16. The cathode was made by depositing a suspension of Fe or Pt carbon nanotubes (CNT) on carbon cloth with ethanol, and the cathode was applied to reduced CO_2 to liquid fuel (isopropanol as the main product) in the gas phase. The simplified process of this reactor was: (1) light passed through the quartz window to reach the photoanode, which in turn generated photogenerated electrons and holes to produce O_2; (2) protons passed through the Nafion membrane, and electrons were collected through the external wire

to reach the cathode; and (3) under the action of the CNT electrocatalyst, electrons and protons reacted with CO_2 to produce liquid fuel, or alternatively, protons and electrons reacted on carbon cloth-supported Pt nanoparticles to produce H_2.
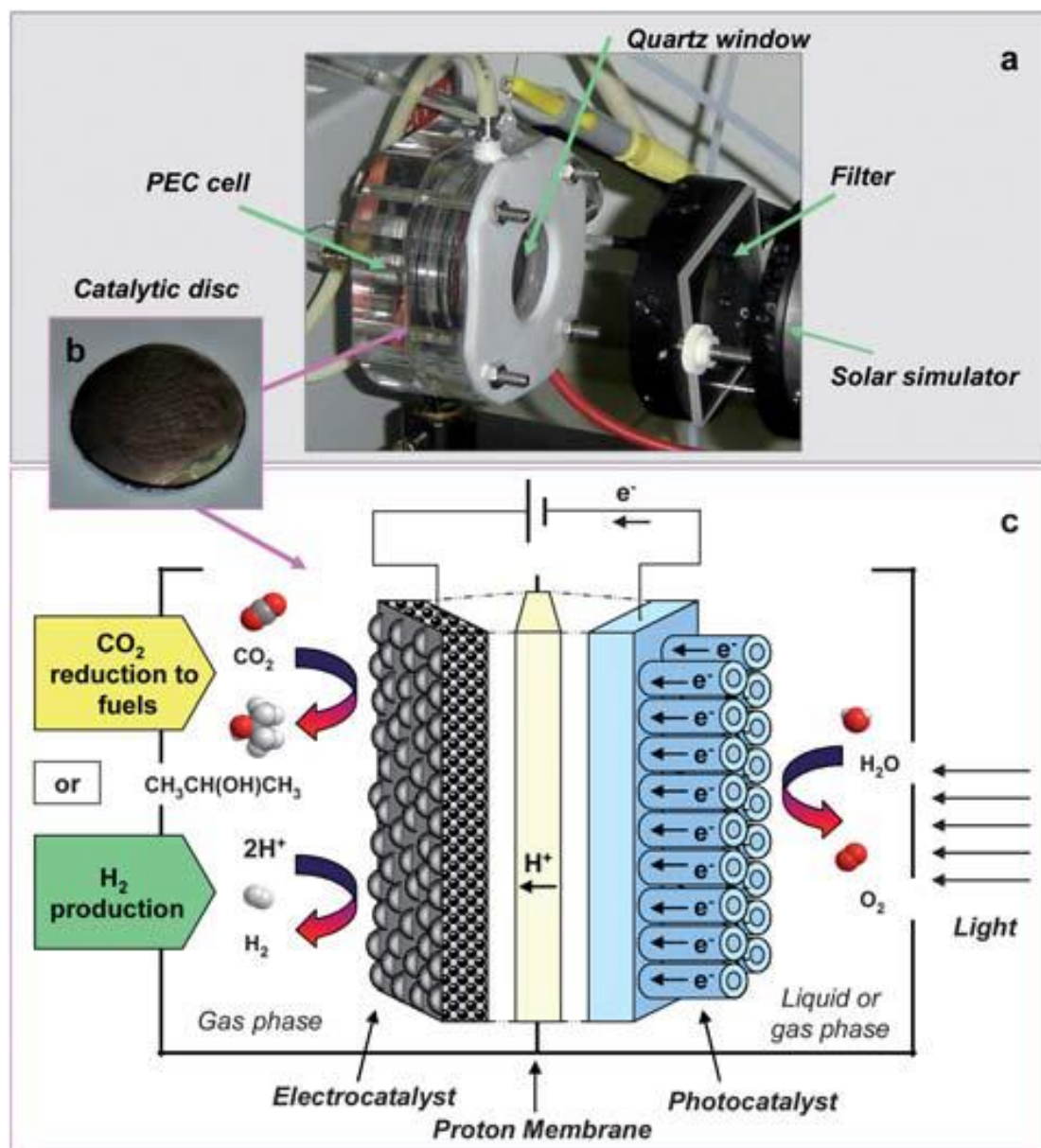

Figure 16. (**a**) View of the lab-scale PEC device. (**b**) Image of the photo/electrocatalytic disc. (**c**) Scheme of the PEC device for CO_2 reduction to fuels and H_2 production. Reprinted from Ref. [150], copyright (2010), with permission from the Royal Society of Chemistry.

Devin et al. reported a microfluidic reactor [151]. It has a structure similar to that of the microfluidic H_2/O_2 fuel cell reported by the group. The cathode and anode of this reactor were separated by a flowing liquid electrolyte [152], and its structure is schematically shown in Figure 17. The study demonstrated that the microfluidic electrochemical cell could be applied as an effective reactor and a versatile analytical tool for the electrochemical reduction of CO_2. The novelty of the design lay in the flowing liquid electrolyte stream, the advantages of which were mainly in the following aspects: (1) the wide flexibility of the working environment, especially in terms of electrolyte composition and pH; (2) the flow of the electrolyte to the anode provided one of the reactants, H_2O, for the reaction

to proceed, while reducing the problem of water management on the electrode surface; (3) the continuous flowing environment facilitated the online collection of samples and allowed for fast and simple analysis of the products; and (4) a reference electrode was placed at the exit stream to promote the analysis of the performance of each electrode. In addition, this cell had a high efficiency (89% response current efficiency and 45% energy efficiency), and its current density reached 100 mA cm^{-2}. Jaramillo et al. designed a CO_2 electroreduction microreactor [153], as shown in Figure 18. The cathode and anode of the reactor were separated by an anion exchange membrane to prevent the interaction of the liquid-phase products of the two poles, and the exit gas was directly passed to the chromatograph for analysis.
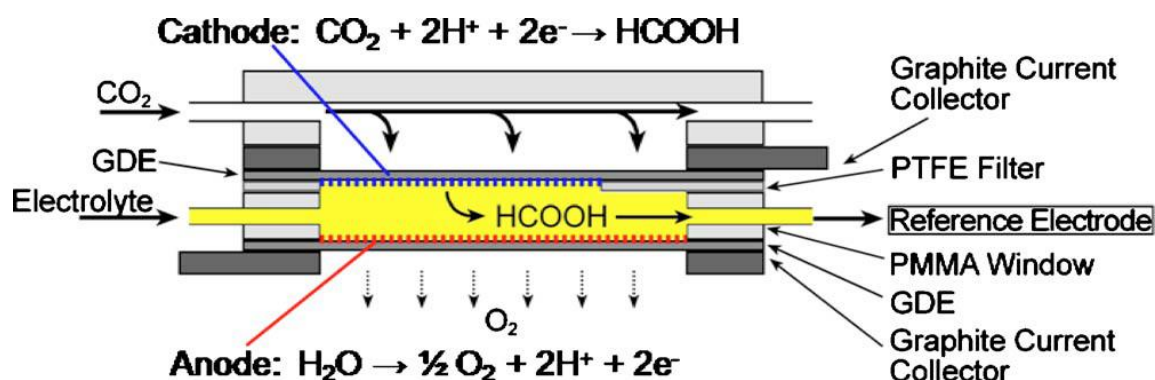
Cathode: $CO_2 + 2H^+ + 2e^- \rightarrow HCOOH$

Anode: $H_2O \rightarrow \frac{1}{2}O_2 + 2H^+ + 2e^-$

Figure 17. Schematic diagram of the microfluidic reactor for CO_2 conversion. Reprinted from Ref. [151], copyright (2010), with permission from the Electrochemical Society.
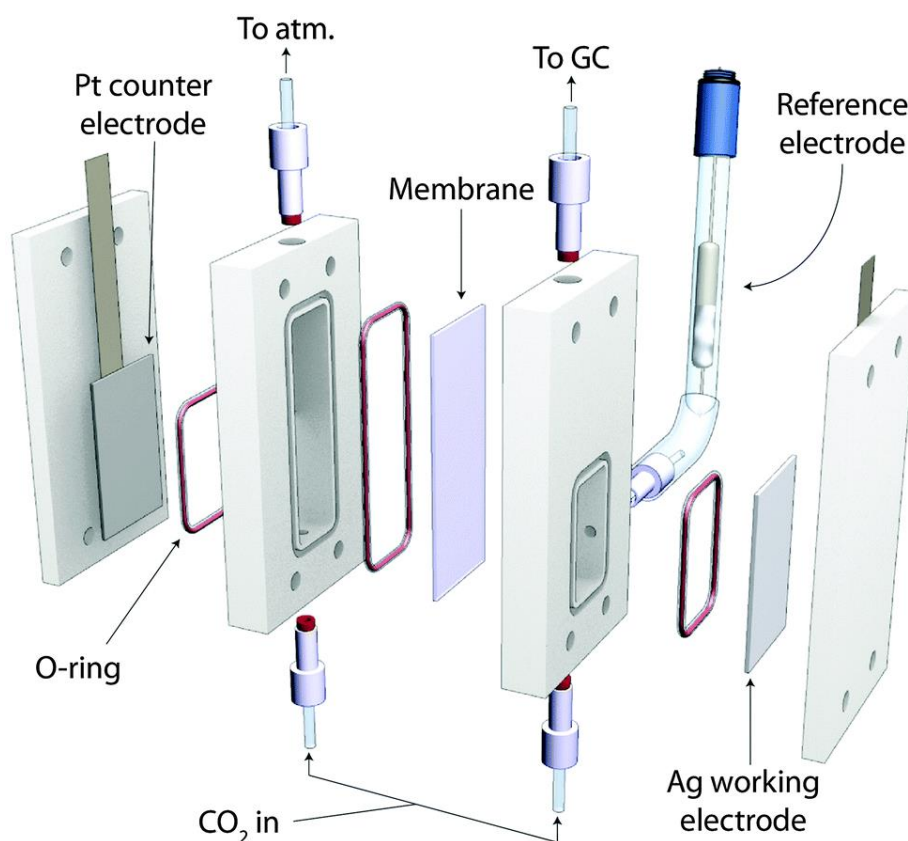

Figure 18. Schematic of the electrochemical cell utilized in this work. Reprinted from Ref. [153], copyright (2014), with permission from the Royal Society of Chemistry.

6. Conclusions and Outlook

The study of electrocatalytic CO_2 reduction is of great importance for spacecraft life support systems and energy storage conversion. However, research on CO_2 electrocatalytic reduction is still at the laboratory stage due to the high overpotential of CO_2 electrocatalytic reduction, the low reduction yield, and the lack of in-depth research on the catalytic mechanism. In order to solve these problems, researchers need to make continuous improvements in catalyst, electrolyte, and reactor design, and explore efficient methods for the electrocatalytic reduction of CO_2.

(1) The core of electrocatalytic CO_2 reduction is how to prepare efficient electrocatalysts that can use their catalytic activity to reduce external electron energy input and energy consumption, while improving the selectivity and controllability of the reduction products. Meanwhile, the catalyst must be able to achieve multielectron and multiproton transfer to enable efficient electrocatalytic reduction of CO_2 on the same surface.

(2) It is necessary to find new electrolyte systems that can synergize with the catalyst in organic systems and to analyze the specific functions of the electrolyte in the electrocatalytic reduction of CO_2 and the mechanism of action in situ in order to better understand the electrocatalytic reduction of CO_2.

(3) Although the design of the reactor is still at a preliminary stage, the size, shape, and structure of the reactor are of great importance to improve the efficiency and selectivity of electrocatalytic CO_2. Therefore, to further promote the practical application of CO_2 electrocatalytic reduction, this research needs to be further strengthened.

In conclusion, as an effective means of CO_2 recycling in space stations, the electrocatalytic reduction of CO_2 has bright research prospects, and this field can further enrich catalytic science and catalytic technology, thus advancing the progress of scientific research in related fields.

References

1. Li, C.; Hu, H.; Yang, M.F.; Pei, Z.Y.; Zhou, Q.; Ren, X.; Liu, B.; Liu, D.; Zeng, X.; Zhang, G.; et al. Characteristics of the lunar samples returned by the Chang'E-5 mission. *Natl. Sci. Rev.* **2022**, *9*, nwab188. [CrossRef]
2. McClean, J.B.; Hoffman, J.A.; Hecht, M.H.; Aboobaker, A.M.; Araghi, K.R.; Elangovan, S.; Graves, C.R.; Hartvigsen, J.J.; Hinterman, E.D.; Liu, A.M. Pre-landing plans for mars oxygen in-situ resource utilization experiment (MOXIE) science operations. *Acta Astronaut.* **2022**, *192*, 301–313. [CrossRef]
3. Schlüter, L.; Cowley, A. Review of techniques for In-Situ oxygen extraction on the moon. *Planet. Space Sci.* **2020**, *181*, 104753. [CrossRef]
4. Kaschubek, D.; Killian, M.; Grill, L. System analysis of a Moon base at the south pole: Considering landing sites, ECLSS and ISRU. *Acta Astronaut.* **2021**, *186*, 33–49. [CrossRef]
5. Starr, S.O.; Muscatello, A.C. Mars in situ resource utilization: A review. *Planet. Space Sci.* **2020**, *182*, 104824. [CrossRef]
6. Chen, H.; du Jonchay, T.S.; Hou, L.; Ho, K. Integrated in-situ resource utilization system design and logistics for Mars exploration. *Acta Astronaut.* **2020**, *170*, 80–92. [CrossRef]
7. Liu, S.; Hu, B.; Zhao, J.; Jiang, W.; Feng, D.; Zhang, C.; Yao, W. Enhanced electrocatalytic CO_2 reduction of bismuth nanosheets with introducing surface bismuth subcarbonate. *Coatings* **2022**, *12*, 233. [CrossRef]
8. Zhang, W.; Hu, Y.; Ma, L.; Zhu, G.; Zhao, P.; Xue, X.; Chen, R.; Yang, S.; Ma, J.; Liu, J. Liquid-phase exfoliated ultrathin Bi nanosheets: Uncovering the origins of enhanced electrocatalytic CO_2 reduction on two-dimensional metal nanostructure. *Nano Energy* **2018**, *53*, 808–816. [CrossRef]

9. Feng, D.; Jiang, W.; Zhang, C.; Li, L.; Hu, B.; Song, J.; Yao, W. A Membrane Reactor with Microchannels for Carbon Dioxide Reduction in Extraterrestrial Space. *Catalysts* **2022**, *12*, 3. [CrossRef]

10. Cestellos-Blanco, S.; Friedline, S.; Sander, K.B.; Abel, A.J.; Kim, J.M.; Clark, D.S.; Arkin, A.P.; Yang, P. Production of PHB from CO_2-derived acetate with minimal processing assessed for space biomanufacturing. *Front. Microbiol.* **2021**, *12*, 700010. [CrossRef]

11. Su, Y.; Cestellos-Blanco, S.; Kim, J.M.; Shen, Y.-X.; Kong, Q.; Lu, D.; Liu, C.; Zhang, H.; Cao, Y.; Yang, P. Close-packed nanowire-bacteria hybrids for efficient solar-driven CO_2 fixation. *Joule* **2020**, *4*, 800–811. [CrossRef]

12. Hecht, M.; Hoffman, J.; Rapp, D.; McClean, J.; SooHoo, J.; Schaefer, R.; Aboobaker, A.; Mellstrom, J.; Hartvigsen, J.; Meyen, F. Mars oxygen ISRU experiment (MOXIE). *Space Sci. Rev.* **2021**, *217*, 1–76. [CrossRef]

13. Calvinho, K.U.; Laursen, A.B.; Yap, K.M.; Goetjen, T.A.; Hwang, S.; Murali, N.; Mejia-Sosa, B.; Lubarski, A.; Teeluck, K.M.; Hall, E.S. Selective CO_2 reduction to C_3 and C_4 oxyhydrocarbons on nickel phosphides at overpotentials as low as 10 mV. *Energy Environ. Sci.* **2018**, *11*, 2550–2559. [CrossRef]

14. da Silva Freitas, W.; D'Epifanio, A.; Mecheri, B. Electrocatalytic CO_2 reduction on nanostructured metal-based materials: Challenges and constraints for a sustainable pathway to decarbonization. *J. CO_2 Util.* **2021**, *50*, 101579. [CrossRef]

15. Casebolt, R.; Levine, K.; Suntivich, J.; Hanrath, T. Pulse check: Potential opportunities in pulsed electrochemical CO_2 reduction. *Joule* **2021**, *5*, 1987–2026. [CrossRef]

16. Chen, J.; Wang, T.; Li, Z.; Yang, B.; Zhang, Q.; Lei, L.; Feng, P.; Hou, Y. Recent progress and perspective of electrochemical CO_2 reduction towards C_2-C_5 products over non-precious metal heterogeneous electrocatalysts. *Nano Res.* **2021**, *14*, 3188–3207. [CrossRef]

17. Chen, Q.; Tsiakaras, P.; Shen, P. Electrochemical Reduction of Carbon Dioxide: Recent Advances on Au-Based Nanocatalysts. *Catalysts* **2022**, *12*, 1348. [CrossRef]

18. Chen, C.; Zhang, Z.; Li, G.; Li, L.; Lin, Z. Recent advances on nanomaterials for electrocatalytic CO_2 conversion. *Energy Fuels* **2021**, *35*, 7485–7510. [CrossRef]

19. Tran, K.; Ulissi, Z.W. Active learning across intermetallics to guide discovery of electrocatalysts for CO_2 reduction and H_2 evolution. *Nat. Catal.* **2018**, *1*, 696–703. [CrossRef]

20. Xie, L.; Liang, J.; Priest, C.; Wang, T.; Ding, D.; Wu, G.; Li, Q. Engineering the atomic arrangement of bimetallic catalysts for electrochemical CO_2 reduction. *Chem. Commun.* **2021**, *57*, 1839–1854. [CrossRef]

21. Giusi, D.; Miceli, M.; Genovese, C.; Centi, G.; Perathoner, S.; Ampelli, C. In situ electrochemical characterization of Cu_xO-based gas-diffusion electrodes (GDEs) for CO_2 electrocatalytic reduction in presence and absence of liquid electrolyte and relationship with C_2+ products formation. *Appl. Catal. B Environ.* **2022**, *318*, 121845. [CrossRef]

22. Yang, K.; Yang, Z.; Zhang, C.; Gu, Y.; Wei, J.; Li, Z.; Ma, C.; Yang, X.; Song, K.; Li, Y. Recent advances in CdS-based photocatalysts for CO_2 photocatalytic conversion. *Chem. Eng. J.* **2021**, *418*, 129344. [CrossRef]

23. Yang, K.D.; Lee, C.W.; Jin, K.; Im, S.W.; Nam, K.T. Current status and bioinspired perspective of electrochemical conversion of CO_2 to a long-chain hydrocarbon. *J. Phys. Chem. Lett.* **2017**, *8*, 538–545. [CrossRef] [PubMed]

24. Khan, I. Strategies for Improved Electrochemical CO_2 Reduction to Value-Added Products by Highly Anticipated Copper-Based Nanoarchitectures. *Chem. Rec.* **2022**, *22*, e202100219. [CrossRef]

25. Fan, Q.; Zhang, M.; Jia, M.; Liu, S.; Qiu, J.; Sun, Z. Electrochemical CO_2 reduction to C_2+ species: Heterogeneous electrocatalysts, reaction pathways, and optimization strategies. *Mater. Today Energy* **2018**, *10*, 280–301. [CrossRef]

26. Zhang, B.; Wang, L.; Li, D.; Li, Z.; Bu, R.; Lu, Y. Tandem strategy for electrochemical CO_2 reduction reaction. *Chem Catal.* **2022**, *2*, 3395–3429. [CrossRef]

27. Zhang, J.; Sewell, C.D.; Huang, H.; Lin, Z. Closing the anthropogenic chemical carbon cycle toward a sustainable future via CO_2 valorization. *Adv. Energy Mater.* **2021**, *11*, 2102767. [CrossRef]

28. Sun, M.; Wong, H.H.; Wu, T.; Dougherty, A.W.; Huang, B. Entanglement of spatial and energy segmentation for C1 pathways in CO_2 reduction on carbon skeleton supported atomic catalysts. *Adv. Energy Mater.* **2022**, *12*, 2103781. [CrossRef]

29. Rehman, A.; Nazir, G.; Rhee, K.Y.; Park, S.-J. Electrocatalytic and photocatalytic sustainable conversion of carbon dioxide to value-added chemicals: State-of-the-art progress, challenges, and future directions. *J. Environ. Chem. Eng.* **2022**, *10*, 108219. [CrossRef]

30. Li, R.; Xiang, K.; Liu, Z.; Peng, Z.; Zou, Y.; Wang, S. Recent Advances in Upgrading of Low-Cost Oxidants to Value-Added Products by Electrocatalytic Reduction Reaction. *Adv. Funct. Mater.* **2022**, *32*, 2208212. [CrossRef]

31. He, C.; Duan, D.; Low, J.; Bai, Y.; Jiang, Y.; Wang, X.; Chen, S.; Long, R.; Song, L.; Xiong, Y. $Cu_{2-x}S$ derived copper nanoparticles: A platform for unraveling the role of surface reconstruction in efficient electrocatalytic CO_2-to-C_2H_4 conversion. *Nano Res.* **2021**, 1–5. [CrossRef]

32. Wijaya, D.T.; Lee, C.W. Metal-Organic framework catalysts: A versatile platform for bioinspired electrochemical conversion of carbon dioxide. *Chem. Eng. J.* **2022**, *446*, 137311. [CrossRef]

33. Franco, F.; Rettenmaier, C.; Jeon, H.S.; Cuenya, B.R. Transition metal-based catalysts for the electrochemical CO_2 reduction: From atoms and molecules to nanostructured materials. *Chem. Soc. Rev.* **2020**, *49*, 6884–6946. [CrossRef]

34. Zhang, J.; Zeng, G.; Chen, L.; Lai, W.; Yuan, Y.; Lu, Y.; Ma, C.; Zhang, W.; Huang, H. Tuning the reaction path of CO_2 electroreduction reaction on indium single-atom catalyst: Insights into the active sites. *Nano Res.* **2022**, *15*, 4014–4022. [CrossRef]

35. Sargeant, E.; Rodríguez, P. Electrochemical conversion of CO_2 in non-conventional electrolytes: Recent achievements and future challenges. *Electrochem. Sci. Adv.* **2022**, e2100178.

36. Cheng, Y.; Wang, H.; Qian, T.; Yan, C. Interfacial engineering of carbon-based materials for efficient electrocatalysis: Recent advances and future. *EnergyChem* **2022**, *4*, 100074. [CrossRef]

37. Shan, J.; Shi, Y.; Li, H.; Chen, Z.; Shuai, Y.; Wang, Z. Effective CO_2 electroreduction toward C_2H_4 boosted by Ce-doped Cu nanoparticles. *Chem. Eng. J.* **2022**, *433*, 133769. [CrossRef]

38. Liu, L.; Li, M.; Chen, F.; Huang, H. Recent Advances on Single-Atom Catalysts for CO_2 Reduction. *Small Struct.* **2022**, *4*, 2200188. [CrossRef]

39. Vinoth, S.; Ong, W.-J.; Pandikumar, A. Defect engineering of BiOX (X= Cl, Br, I) based photocatalysts for energy and environmental applications: Current progress and future perspectives. *Coord. Chem. Rev.* **2022**, *464*, 214541. [CrossRef]

40. Yan, Z.; Wu, T. Highly Selective Electrochemical CO_2 Reduction to C_2 Products on a g-C_3N_4-Supported Copper-Based Catalyst. *Int. J. Mol. Sci.* **2022**, *23*, 14381. [CrossRef]

41. Garba, M.D.; Usman, M.; Khan, S.; Shehzad, F.; Galadima, A.; Ehsan, M.F.; Ghanem, A.S.; Humayun, M. CO_2 towards fuels: A review of catalytic conversion of carbon dioxide to hydrocarbons. *J. Environ. Chem. Eng.* **2021**, *9*, 104756. [CrossRef]

42. Sa, Y.J.; Lee, C.W.; Lee, S.Y.; Na, J.; Lee, U.; Hwang, Y.J. Catalyst–electrolyte interface chemistry for electrochemical CO_2 reduction. *Chem. Soc. Rev.* **2020**, *49*, 6632–6665. [CrossRef]

43. Li, X.; Yu, J.; Jaroniec, M.; Chen, X. Cocatalysts for selective photoreduction of CO_2 into solar fuels. *Chem. Rev.* **2019**, *119*, 3962–4179. [CrossRef] [PubMed]

44. Deng, B.; Huang, M.; Zhao, X.; Mou, S.; Dong, F. Interfacial electrolyte effects on electrocatalytic CO_2 reduction. *ACS Catal.* **2021**, *12*, 331–362. [CrossRef]

45. Qiao, J.; Liu, Y.; Hong, F.; Zhang, J. A review of catalysts for the electroreduction of carbon dioxide to produce low-carbon fuels. *Chem. Soc. Rev.* **2014**, *43*, 631–675. [CrossRef]

46. Neyrizi, S.; Kiewiet, J.; Hempenius, M.A.; Mul, G. What It Takes for Imidazolium Cations to Promote Electrochemical Reduction of CO_2. *ACS Energy Lett.* **2022**, *7*, 3439–3446. [CrossRef]

47. Salimijazi, F.; Kim, J.; Schmitz, A.M.; Grenville, R.; Bocarsly, A.; Barstow, B. Constraints on the efficiency of engineered electromicrobial production. *Joule* **2020**, *4*, 2101–2130. [CrossRef]

48. Tahir, M.; Ali Khan, A.; Tasleem, S.; Mansoor, R.; Fan, W.K. Titanium carbide (Ti_3C_2) MXene as a promising co-catalyst for photocatalytic CO_2 conversion to energy-efficient fuels: A review. *Energy Fuels* **2021**, *35*, 10374–10404. [CrossRef]

49. Gunasekar, G.H.; Park, K.; Jung, K.-D.; Yoon, S. Recent developments in the catalytic hydrogenation of CO_2 to formic acid/formate using heterogeneous catalysts. *Inorg. Chem. Front.* **2016**, *3*, 882–895. [CrossRef]

50. Papasizza, M.; Yang, X.; Cheng, J.; Cuesta, A. Electrocatalytic reduction of CO_2 in neat and water-containing imidazolium-based ionic liquids. *Curr. Opin. Electrochem.* **2020**, *23*, 80–88. [CrossRef]

51. Ma, Z.; Wan, T.; Zhang, D.; Yuwono, J.A.; Tsounis, C.; Jiang, J.; Chou, Y.-H.; Lu, X.; Kumar, P.V.; Ng, Y.H. Atomically Dispersed Cu Catalysts on Sulfide-Derived Defective Ag Nanowires for Electrochemical CO_2 Reduction. *ACS Nano* **2023**, *17*, 2387–2398. [CrossRef]

52. Al Sadat, W.I.; Archer, L.A. The O_2-assisted Al/CO_2 electrochemical cell: A system for CO_2 capture/conversion and electric power generation. *Sci. Adv.* **2016**, *2*, e1600968. [CrossRef] [PubMed]

53. Huang, Y.G.; Wu, S.Q.; Deng, W.H.; Xu, G.; Hu, F.L.; Hill, J.P.; Wei, W.; Su, S.Q.; Shrestha, L.K.; Sato, O. Selective CO_2 capture and high proton conductivity of a functional star-of-david catenane metal–organic framework. *Adv. Mater.* **2017**, *29*, 1703301. [CrossRef] [PubMed]

54. Chung, D.Y.; Jun, S.W.; Yoon, G.; Kwon, S.G.; Shin, D.Y.; Seo, P.; Yoo, J.M.; Shin, H.; Chung, Y.-H.; Kim, H. Highly durable and active PtFe nanocatalyst for electrochemical oxygen reduction reaction. *J. Am. Chem. Soc.* **2015**, *137*, 15478–15485. [CrossRef]

55. Fu, J.; Liu, K.; Li, H.; Hu, J.; Liu, M. Bimetallic atomic site catalysts for CO_2 reduction reactions: A review. *Environ. Chem. Lett.* **2022**, *20*, 243–262. [CrossRef]

56. Giannakoudakis, D.A.; Colmenares, J.C.; Tsiplakides, D.; Triantafyllidis, K.S. Nanoengineered electrodes for biomass-derived 5-hydroxymethylfurfural electrocatalytic oxidation to 2,5-furandicarboxylic acid. *ACS Sustain. Chem. Eng.* **2021**, *9*, 1970–1993. [CrossRef]

57. Liang, B.; Zhao, Y.; Yang, J. Recent advances in developing artificial autotrophic microorganism for reinforcing CO_2 fixation. *Front. Microbiol.* **2020**, *11*, 592631. [CrossRef]

58. Feng, J.; Zeng, S.; Feng, J.; Dong, H.; Zhang, X. CO_2 electroreduction in ionic liquids: A review. *Chin. J. Chem.* **2018**, *36*, 961–970. [CrossRef]

59. Guan, Y.; Liu, M.; Rao, X.; Liu, Y.; Zhang, J. Electrochemical reduction of carbon dioxide (CO_2): Bismuth-based electrocatalysts. *J. Mater. Chem. A* **2021**, *9*, 13770–13803. [CrossRef]

60. Zhang, L.; Zhao, Z.J.; Gong, J. Nanostructured materials for heterogeneous electrocatalytic CO_2 reduction and their related reaction mechanisms. *Angew. Chem. Int. Ed.* **2017**, *56*, 11326–11353. [CrossRef]

61. Zhu, D.D.; Liu, J.L.; Qiao, S.Z. Recent advances in inorganic heterogeneous electrocatalysts for reduction of carbon dioxide. *Adv. Mater.* **2016**, *28*, 3423–3452. [CrossRef] [PubMed]

62. Li, X.; Yang, X.; Xue, H.; Pang, H.; Xu, Q. Metal–organic frameworks as a platform for clean energy applications. *EnergyChem* **2020**, *2*, 100027. [CrossRef]

63. Qin, S.; Ge, C.; Kong, X.; Fu, M.; Zhuang, Z.; Li, X. Photothermal Catalytic Reduction of CO_2 by Cobalt Silicate Heterojunction Constructed from Clay Minerals. *Catalysts* **2022**, *13*, 32. [CrossRef]

64. Zhang, Y.; Dong, L.-Z.; Li, S.; Huang, X.; Chang, J.-N.; Wang, J.-H.; Zhou, J.; Li, S.-L.; Lan, Y.-Q. Coordination environment dependent selectivity of single-site-Cu enriched crystalline porous catalysts in CO_2 reduction to CH_4. *Nat. Commun.* **2021**, *12*, 6390. [CrossRef] [PubMed]

65. Zhou, H.; Yan, R.; Zhang, D.; Fan, T. Challenges and perspectives in designing artificial photosynthetic systems. *Chem. Eur. J.* **2016**, *22*, 9870–9885. [CrossRef] [PubMed]

66. Wang, Y.; Zheng, M.; Wang, X.; Zhou, X. Electrocatalytic Reduction of CO_2 to C_1 Compounds by Zn-Based Monatomic Alloys: A DFT Calculation. *Catalysts* **2022**, *12*, 1617. [CrossRef]

67. Taheri, A.; Berben, L.A. Making C–H bonds with CO_2: Production of formate by molecular electrocatalysts. *Chem. Commun.* **2016**, *52*, 1768–1777. [CrossRef]

68. Jouny, M.; Lv, J.-J.; Cheng, T.; Ko, B.H.; Zhu, J.-J.; Goddard III, W.A.; Jiao, F. Formation of carbon–nitrogen bonds in carbon monoxide electrolysis. *Nat. Chem.* **2019**, *11*, 846–851. [CrossRef]

69. Yang, N.; Waldvogel, S.R.; Jiang, X. Electrochemistry of carbon dioxide on carbon electrodes. *ACS Appl. Mater. Interfaces* **2016**, *8*, 28357–28371. [CrossRef]

70. Di, Z.; Qi, Y.; Yu, X.; Hu, F. The Progress of Metal-Organic Framework for Boosting CO_2 Conversion. *Catalysts* **2022**, *12*, 1582. [CrossRef]

71. Yoo, C.J.; Dong, W.J.; Park, J.Y.; Lim, J.W.; Kim, S.; Choi, K.S.; Odongo Ngome, F.O.; Choi, S.-Y.; Lee, J.-L. Compositional and geometrical effects of bimetallic Cu–Sn catalysts on selective electrochemical CO_2 reduction to CO. *ACS Appl. Energy Mater.* **2020**, *3*, 4466–4473. [CrossRef]

72. Matavos-Aramyan, S.; Soukhakian, S.; Jazebizadeh, M.H.; Moussavi, M.; Hojjati, M.R. On engineering strategies for photoselective CO_2 reduction–A thorough review. *Appl. Mater. Today* **2020**, *18*, 100499. [CrossRef]

73. Wang, F. Artificial photosynthetic systems for CO_2 reduction: Progress on higher efficiency with cobalt complexes as catalysts. *ChemSusChem* **2017**, *10*, 4393–4402. [CrossRef] [PubMed]

74. Govindan, B.; Madhu, R.; Abu Haija, M.; Kusmartsev, F.V.; Banat, F. Pd-Decorated 2D MXene (2D $Ti_3C_2Ti_x$) as a High-Performance Electrocatalyst for Reduction of Carbon Dioxide into Fuels toward Climate Change Mitigation. *Catalysts* **2022**, *12*, 1180. [CrossRef]

75. Mostafa, M.M.M.; Bajafar, W.; Gu, L.; Narasimharao, K.; Abdel Salam, M.; Alshehri, A.; Khdary, N.H.; Al-Faifi, S.; Chowdhury, A.D. Electrochemical Characteristics of Nanosized Cu, Ni, and Zn Cobaltite Spinel Materials. *Catalysts* **2022**, *12*, 893. [CrossRef]

76. Li, X.; Chang, S.; Wang, Y.; Zhang, L. Silver-Carbonaceous Microsphere Precursor-Derived Nano-Coral Ag Catalyst for Electro-chemical Carbon Dioxide Reduction. *Catalysts* **2022**, *12*, 479. [CrossRef]

77. Costentin, C.; Drouet, S.; Robert, M.; Savéant, J.-M. A local proton source enhances CO_2 electroreduction to CO by a molecular Fe catalyst. *Science* **2012**, *338*, 90–94. [CrossRef]

78. Angamuthu, R.; Byers, P.; Lutz, M.; Spek, A.L.; Bouwman, E. Electrocatalytic CO_2 conversion to oxalate by a copper complex. *Science* **2010**, *327*, 313–315. [CrossRef]

79. Hoffman, Z.B.; Gray, T.S.; Moraveck, K.B.; Gunnoe, T.B.; Zangari, G. Electrochemical reduction of carbon dioxide to syngas and formate at dendritic copper–indium electrocatalysts. *ACS Catal.* **2017**, *7*, 5381–5390. [CrossRef]

80. Zhao, Z.; Peng, X.; Liu, X.; Sun, X.; Shi, J.; Han, L.; Li, G.; Luo, J. Efficient and stable electroreduction of CO_2 to CH_4 on CuS nanosheet arrays. *J. Mater. Chem. A* **2017**, *5*, 20239–20243. [CrossRef]

81. Huang, J.; Hu, Q.; Guo, X.; Zeng, Q.; Wang, L. Rethinking $Co(CO_3)_{0.5}(OH)\cdot0.11H_2O$: A new property for highly selective electrochemical reduction of carbon dioxide to methanol in aqueous solution. *Green Chem.* **2018**, *20*, 2967–2972. [CrossRef]

82. Wang, X.; Chen, Z.; Zhao, X.; Yao, T.; Chen, W.; You, R.; Zhao, C.; Wu, G.; Wang, J.; Huang, W. Regulation of coordination number over single Co sites: Triggering the efficient electroreduction of CO_2. *Angew. Chem.* **2018**, *130*, 1962–1966. [CrossRef]

83. Zhu, W.; Zhang, L.; Yang, P.; Hu, C.; Luo, Z.; Chang, X.; Zhao, Z.J.; Gong, J. Low-coordinated edge sites on ultrathin palladium nanosheets boost carbon dioxide electroreduction performance. *Angew. Chem. Int. Ed.* **2018**, *57*, 11544–11548. [CrossRef] [PubMed]

84. Zhang, A.; Liang, Y.; Li, H.; Zhao, X.; Chen, Y.; Zhang, B.; Zhu, W.; Zeng, J. Harmonizing the electronic structures of the adsorbate and catalysts for efficient CO_2 reduction. *Nano Lett.* **2019**, *19*, 6547–6553. [CrossRef]

85. Jiang, H.; Gong, Y.; Jiao, L.; Qian, Y.; Pan, C.; Zheng, L.; Cai, X.; Liu, B.; Yu, S. Regulating coordination environment of single-atom Ni electrocatalysts templated by MOF for boosting CO_2 reduction. *Angew. Chem. Int. Ed* **2019**, *59*, 2705–2709.

86. Ren, W.; Tan, X.; Yang, W.; Jia, C.; Xu, S.; Wang, K.; Smith, S.C.; Zhao, C. Isolated diatomic Ni-Fe metal–nitrogen sites for synergistic electroreduction of CO_2. *Angew. Chem. Int. Ed.* **2019**, *58*, 6972–6976. [CrossRef]

87. Wang, Y.; Cao, L.; Libretto, N.J.; Li, X.; Li, C.; Wan, Y.; He, C.; Lee, J.; Gregg, J.; Zong, H. Ensemble effect in bimetallic electrocatalysts for CO_2 reduction. *J. Am. Chem. Soc.* **2019**, *141*, 16635–16642. [CrossRef]

88. Pan, J.; Sun, Y.; Deng, P.; Yang, F.; Chen, S.; Zhou, Q.; Park, H.S.; Liu, H.; Xia, B.Y. Hierarchical and ultrathin copper nanosheets synthesized via galvanic replacement for selective electrocatalytic carbon dioxide conversion to carbon monoxide. *Appl. Catal. B Environ.* **2019**, *255*, 117736. [CrossRef]

89. Wang, Y.; Shen, H.; Livi, K.J.; Raciti, D.; Zong, H.; Gregg, J.; Onadeko, M.; Wan, Y.; Watson, A.; Wang, C. Copper nanocubes for CO_2 reduction in gas diffusion electrodes. *Nano Lett.* **2019**, *19*, 8461–8468. [CrossRef]

90. Zhang, H.; Li, J.; Xi, S.; Du, Y.; Hai, X.; Wang, J.; Xu, H.; Wu, G.; Zhang, J.; Lu, J. A graphene-supported single-atom FeN_5 catalytic site for efficient electrochemical CO_2 reduction. *Angew. Chem.* **2019**, *131*, 15013–15018. [CrossRef]

91.   Zhang, Z.; Ma, C.; Tu, Y.; Si, R.; Wei, J.; Zhang, S.; Wang, Z.; Li, J.-F.; Wang, Y.; Deng, D. Multiscale carbon foam confining single iron atoms for efficient electrocatalytic CO_2 reduction to CO. *Nano Res.* **2019**, *12*, 2313–2317. [CrossRef]

92.   Gu, J.; Hsu, C.-S.; Bai, L.; Chen, H.M.; Hu, X. Atomically dispersed Fe^{3+} sites catalyze efficient CO_2 electroreduction to CO. *Science* **2019**, *364*, 1091–1094. [CrossRef] [PubMed]

93.   Zhao, S.; Chen, G.; Zhou, G.; Yin, L.C.; Veder, J.P.; Johannessen, B.; Saunders, M.; Yang, S.Z.; De Marco, R.; Liu, C. A universal seeding strategy to synthesize single atom catalysts on 2D materials for electrocatalytic applications. *Adv. Funct. Mater.* **2020**, *30*, 1906157. [CrossRef]

94.   Liu, S.; Yang, H.B.; Hung, S.F.; Ding, J.; Cai, W.; Liu, L.; Gao, J.; Li, X.; Ren, X.; Kuang, Z. Elucidating the electrocatalytic CO_2 reduction reaction over a model single-atom nickel catalyst. *Angew. Chem. Int. Ed.* **2020**, *59*, 798–803. [CrossRef]

95.   Gong, Y.N.; Jiao, L.; Qian, Y.; Pan, C.Y.; Zheng, L.; Cai, X.; Liu, B.; Yu, S.H.; Jiang, H.L. Regulating the coordination environment of MOF-templated single-atom nickel electrocatalysts for boosting CO_2 reduction. *Angew. Chem.* **2020**, *132*, 2727–2731. [CrossRef]

96.   Zhang, A.; Liang, Y.; Li, H.; Zhang, B.; Liu, Z.; Chang, Q.; Zhang, H.; Zhu, C.-F.; Geng, Z.; Zhu, W. In-situ surface reconstruction of InN nanosheets for efficient CO_2 electroreduction into formate. *Nano Lett.* **2020**, *20*, 8229–8235. [CrossRef]

97.   Xie, W.; Li, H.; Cui, G.; Li, J.; Song, Y.; Li, S.; Zhang, X.; Lee, J.Y.; Shao, M.; Wei, M. NiSn atomic pair on an integrated electrode for synergistic electrocatalytic CO_2 reduction. *Angew. Chem.* **2021**, *133*, 7458–7464. [CrossRef]

98.   Guo, J.-H.; Zhang, X.-Y.; Dao, X.-Y.; Sun, W.-Y. Nanoporous metal–organic framework-based ellipsoidal nanoparticles for the catalytic electroreduction of CO_2. *ACS Appl. Nano Mater.* **2020**, *3*, 2625–2635. [CrossRef]

99.   Zhong, M.; Tran, K.; Min, Y.; Wang, C.; Wang, Z.; Dinh, C.-T.; De Luna, P.; Yu, Z.; Rasouli, A.S.; Brodersen, P. Accelerated discovery of CO_2 electrocatalysts using active machine learning. *Nature* **2020**, *581*, 178–183. [CrossRef] [PubMed]

100.   Huang, Y.; Mao, X.; Yuan, G.; Zhang, D.; Pan, B.; Deng, J.; Shi, Y.; Han, N.; Li, C.; Zhang, L. Size-dependent selectivity of electrochemical CO_2 reduction on converted In_2O_3 nanocrystals. *Angew. Chem.* **2021**, *133*, 15978–15982. [CrossRef]

101.   Li, J.; Zhang, Z.; Hu, W. Exclusive CO_2-to-formate conversion over single-atom alloyed Cu-based catalysts. *Green Energy Environ.* **2022**, *7*, 855–857. [CrossRef]

102.   Zhang, S.; Mo, Z.; Wang, J.; Liu, H.; Liu, P.; Hu, D.; Tan, T.; Wang, C. Ultra-stable oxygen species in Ag nanoparticles anchored on g-C3N4 for enhanced electrochemical reduction of CO_2. *Electrochim. Acta* **2021**, *390*, 138831. [CrossRef]

103.   Zhao, Y.; Miao, Z.; Wang, F.; Liang, M.; Liu, Y.; Wu, M.; Diao, L.; Mu, J.; Cheng, Y.; Zhou, J. N-doped carbon-encapsulated nickel on reduced graphene oxide materials for efficient CO_2 electroreduction to syngas with potential-independent H_2/CO ratios. *J. Environ. Chem. Eng.* **2021**, *9*, 105515. [CrossRef]

104.   Wang, X.; Liu, S.; Zhang, H.; Zhang, S.; Meng, G.; Liu, Q.; Sun, Z.; Luo, J.; Liu, X. Polycrystalline SnS_x nanofilm enables CO_2 electroreduction to formate with high current density. *Chem. Commun.* **2022**, *58*, 7654–7657. [CrossRef]

105.   Zhai, J.; Kang, Q.; Liu, Q.; Lai, D.; Lu, Q.; Gao, F. In-situ generation of In_2O_3 nanoparticles inside In [Co(CN)$_6$] quasi-metal-organic-framework nanocubes for efficient electroreduction of CO_2 to formate. *J. Colloid Interface Sci.* **2022**, *608*, 1942–1950. [CrossRef] [PubMed]

106.   Jiang, Z.; Wang, T.; Pei, J.; Shang, H.; Zhou, D.; Li, H.; Dong, J.; Wang, Y.; Cao, R.; Zhuang, Z. Discovery of main group single Sb–N$_4$ active sites for CO_2 electroreduction to formate with high efficiency. *Energy Environ. Sci.* **2020**, *13*, 2856–2863. [CrossRef]

107.   Gao, S.; Wang, T.; Jin, M.; Zhang, S.; Liu, Q.; Hu, G.; Yang, H.; Luo, J.; Liu, X. Bifunctional Nb-NC atomic catalyst for aqueous Zn-air battery driving CO_2 electrolysis. *Sci. China Mater.* **2022**, *66*, 1013–1023.

108.   Peterson, A.A.; Abild-Pedersen, F.; Studt, F.; Rossmeisl, J.; Nørskov, J.K. How copper catalyzes the electroreduction of carbon dioxide into hydrocarbon fuels. *Energy Environ. Sci.* **2010**, *3*, 1311–1315. [CrossRef]

109.   Li, C.W.; Kanan, M.W. CO_2 reduction at low overpotential on Cu electrodes resulting from the reduction of thick Cu_2O films. *J. Am. Chem. Soc.* **2012**, *134*, 7231–7234. [CrossRef]

110.   Guo, X.; Zhang, Y.; Deng, C.; Li, X.; Xue, Y.; Yan, Y.-M.; Sun, K. Composition dependent activity of Cu–Pt nanocrystals for electrochemical reduction of CO_2. *Chem. Commun.* **2015**, *51*, 1345–1348. [CrossRef]

111.   Ni, W.; Li, C.; Zang, X.; Xu, M.; Huo, S.; Liu, M.; Yang, Z.; Yan, Y.-M. Efficient electrocatalytic reduction of CO_2 on CuxO decorated graphene oxides: An insight into the role of multivalent Cu in selectivity and durability. *Appl. Catal. B Environ.* **2019**, *259*, 118044. [CrossRef]

112.   Chen, Y.; Li, C.W.; Kanan, M.W. Aqueous CO_2 reduction at very low overpotential on oxide-derived Au nanoparticles. *J. Am. Chem. Soc.* **2012**, *134*, 19969–19972. [CrossRef] [PubMed]

113.   Gao, D.; Zhou, H.; Wang, J.; Miao, S.; Yang, F.; Wang, G.; Wang, J.; Bao, X. Size-dependent electrocatalytic reduction of CO_2 over Pd nanoparticles. *J. Am. Chem. Soc.* **2015**, *137*, 4288–4291. [CrossRef] [PubMed]

114.   Li, S.; Dong, X.; Chen, W.; Song, Y.; Li, G.; Wei, W.; Sun, Y. Efficient CO_2 Electroreduction over Silver Hollow Fiber Electrode. *Catalysts* **2022**, *12*, 453. [CrossRef]

115.   Chen, X.; Wang, H.; Wang, Y.; Bai, Q.; Gao, Y.; Zhang, Z. Synthesis and electrocatalytic performance of multi-component nanoporous PtRuCuW alloy for direct methanol fuel cells. *Catalysts* **2015**, *5*, 1003–1015. [CrossRef]

116.   Zhang, Y.-H.; Liu, M.-M.; Chen, J.-L.; Fang, S.-M.; Zhou, P.-P. Recent advances in Cu_2O-based composites for photocatalysis: A review. *Dalton Trans.* **2021**, *50*, 4091–4111. [CrossRef]

117.   Niu, Z.-Z.; Gao, F.-Y.; Zhang, X.-L.; Yang, P.-P.; Liu, R.; Chi, L.-P.; Wu, Z.-Z.; Qin, S.; Yu, X.; Gao, M.-R. Hierarchical copper with inherent hydrophobicity mitigates electrode flooding for high-rate CO_2 electroreduction to multicarbon products. *J. Am. Chem. Soc.* **2021**, *143*, 8011–8021. [CrossRef]

118. Halder, A.; Curtiss, L.A.; Fortunelli, A.; Vajda, S. Perspective: Size selected clusters for catalysis and electrochemistry. *J. Chem. Phys.* **2018**, *148*, 110901. [CrossRef]

119. Cao, T.; Lin, R.; Liu, S.; Cheong, W.-C.M.; Li, Z.; Wu, K.; Zhu, Y.; Wang, X.; Zhang, J.; Li, Q. Atomically dispersed Ni anchored on polymer-derived mesh-like N-doped carbon nanofibers as an efficient CO_2 electrocatalytic reduction catalyst. *Nano Res.* **2022**, *15*, 3959–3963. [CrossRef]

120. Azhari, N.J.; Nurdini, N.; Mardiana, S.; Ilmi, T.; Fajar, A.T.; Makertihartha, I.; Kadja, G.T. Zeolite-based catalyst for direct conversion of CO_2 to C_2+ hydrocarbon: A review. *J. CO_2 Util.* **2022**, *59*, 101969. [CrossRef]

121. Choukroun, D.; Daems, N.; Kenis, T.; Van Everbroeck, T.; Hereijgers, J.; Altantzis, T.; Bals, S.; Cool, P.; Breugelmans, T. Bifunctional nickel–nitrogen-doped-carbon-supported copper electrocatalyst for CO_2 reduction. *J. Phys. Chem. C* **2020**, *124*, 1369–1381. [CrossRef]

122. Cho, J.H.; Lee, C.; Hong, S.H.; Jang, H.Y.; Back, S.; Seo, M.g.; Lee, M.; Min, H.K.; Choi, Y.; Jang, Y.J. Transition Metal Ion Doping on ZIF-8 for Enhanced the Electrochemical CO_2 Reduction Reaction. *Adv. Mater.* **2022**, 2208224. [CrossRef] [PubMed]

123. Zha, B.; Li, C.; Li, J. Efficient electrochemical reduction of CO_2 into formate and acetate in polyoxometalate catholyte with indium catalyst. *J. Catal.* **2020**, *382*, 69–76. [CrossRef]

124. Gao, S.; Lin, Y.; Jiao, X.; Sun, Y.; Luo, Q.; Zhang, W.; Li, D.; Yang, J.; Xie, Y. Partially oxidized atomic cobalt layers for carbon dioxide electroreduction to liquid fuel. *Nature* **2016**, *529*, 68–71. [CrossRef] [PubMed]

125. Bhugun, I.; Lexa, D.; Saveant, J.-M. Ultraefficient selective homogeneous catalysis of the electrochemical reduction of carbon dioxide by an iron (0) porphyrin associated with a weak Broensted acid cocatalyst. *J. Am. Chem. Soc.* **1994**, *116*, 5015–5016. [CrossRef]

126. Leung, K.; Nielsen, I.M.; Sai, N.; Medforth, C.; Shelnutt, J.A. Cobalt− porphyrin catalyzed electrochemical reduction of carbon dioxide in water. 2. mechanism from first principles. *J. Phys. Chem. A* **2010**, *114*, 10174–10184. [CrossRef]

127. Tornow, C.E.; Thorson, M.R.; Ma, S.; Gewirth, A.A.; Kenis, P.J. Nitrogen-based catalysts for the electrochemical reduction of CO_2 to CO. *J. Am. Chem. Soc.* **2012**, *134*, 19520–19523. [CrossRef]

128. Agarwal, J.; Johnson, R.P.; Li, G. Reduction of CO_2 on a tricarbonyl rhenium (I) complex: Modeling a catalytic cycle. *J. Phys. Chem. A* **2011**, *115*, 2877–2881. [CrossRef]

129. Centi, G.; Quadrelli, E.A.; Perathoner, S. Catalysis for CO_2 conversion: A key technology for rapid introduction of renewable energy in the value chain of chemical industries. *Energy Environ. Sci.* **2013**, *6*, 1711–1731. [CrossRef]

130. Dominguez-Ramos, A.; Irabien, A. The carbon footprint of Power-to-Synthetic Natural Gas by Photovoltaic solar powered Electrochemical Reduction of CO_2. *Sustain. Prod. Consum.* **2019**, *17*, 229–240. [CrossRef]

131. Lo, A.-Y.; Taghipour, F. Review and prospects of microporous zeolite catalysts for CO_2 photoreduction. *Appl. Mater. Today* **2021**, *23*, 101042. [CrossRef]

132. Mota-Lima, A. The electrified plasma/liquid interface as a platform for highly efficient CO_2 electroreduction to oxalate. *J. Phys. Chem. C* **2020**, *124*, 10907–10915. [CrossRef]

133. Golru, S.S.; Biddinger, E.J. Effect of additives in aqueous electrolytes on CO_2 electroreduction. *Chem. Eng. J.* **2022**, *428*, 131303. [CrossRef]

134. Schizodimou, A.; Kyriacou, G. Acceleration of the reduction of carbon dioxide in the presence of multivalent cations. *Electrochim. Acta* **2012**, *78*, 171–176. [CrossRef]

135. Jung, H.; Lee, S.Y.; Lee, C.W.; Cho, M.K.; Won, D.H.; Kim, C.; Oh, H.-S.; Min, B.K.; Hwang, Y.J. Electrochemical fragmentation of Cu_2O nanoparticles enhancing selective C–C coupling from CO_2 reduction reaction. *J. Am. Chem. Soc.* **2019**, *141*, 4624–4633. [CrossRef]

136. Leung, C.-F.; Ho, P.-Y. Molecular catalysis for utilizing CO_2 in fuel electro-generation and in chemical feedstock. *Catalysts* **2019**, *9*, 760. [CrossRef]

137. Shao, X.; Zhang, X.; Liu, Y.; Qiao, J.; Zhou, X.-D.; Xu, N.; Malcombe, J.L.; Yi, J.; Zhang, J. Metal chalcogenide-associated catalysts enabling CO_2 electroreduction to produce low-carbon fuels for energy storage and emission reduction: Catalyst structure, morphology, performance, and mechanism. *J. Mater. Chem. A* **2021**, *9*, 2526–2559. [CrossRef]

138. Zeng, F.; Mebrahtu, C.; Xi, X.; Liao, L.; Ren, J.; Xie, J.; Heeres, H.J.; Palkovits, R. Catalysts design for higher alcohols synthesis by CO_2 hydrogenation: Trends and future perspectives. *Appl. Catal. B Environ.* **2021**, *291*, 120073. [CrossRef]

139. Dokania, A.; Ramirez, A.; Bavykina, A.; Gascon, J. Heterogeneous catalysis for the valorization of CO_2: Role of bifunctional processes in the production of chemicals. *ACS Energy Lett.* **2018**, *4*, 167–176. [CrossRef]

140. Zignani, S.C.; Lo Faro, M.; Palella, A.; Spadaro, L.; Trocino, S.; Lo Vecchio, C.; Aricò, A.S. Bifunctional CuO-Ag/KB Catalyst for the Electrochemical Reduction of CO_2 in an Alkaline Solid-State Electrolysis Cell. *Catalysts* **2022**, *12*, 293. [CrossRef]

141. Ogura, K.; Ferrell III, J.R.; Cugini, A.V.; Smotkin, E.S.; Salazar-Villalpando, M.D. CO_2 attraction by specifically adsorbed anions and subsequent accelerated electrochemical reduction. *Electrochim. Acta* **2010**, *56*, 381–386. [CrossRef]

142. Smieja, J.M.; Sampson, M.D.; Grice, K.A.; Benson, E.E.; Froehlich, J.D.; Kubiak, C.P. Manganese as a substitute for rhenium in CO_2 reduction catalysts: The importance of acids. *Inorg. Chem.* **2013**, *52*, 2484–2491. [CrossRef]

143. Yoshida, T.; Kamato, K.; Tsukamoto, M.; Iida, T.; Schlettwein, D.; Wöhrle, D.; Kaneko, M. Selective electroacatalysis for CO_2 reduction in the aqueous phase using cobalt phthalocyanine/poly-4-vinylpyridine modified electrodes. *J. Electroanal. Chem.* **1995**, *385*, 209–225. [CrossRef]

144. Woo, S.-J.; Choi, S.; Kim, S.-Y.; Kim, P.S.; Jo, J.H.; Kim, C.H.; Son, H.-J.; Pac, C.; Kang, S.O. Highly selective and durable photochemical CO_2 reduction by molecular Mn (I) catalyst fixed on a particular dye-sensitized TiO_2 platform. *ACS Catal.* **2019**, *9*, 2580–2593. [CrossRef]

145. Martindale, B.C.; Compton, R.G. Formic acid electro-synthesis from carbon dioxide in a room temperature ionic liquid. *Chem. Commun.* **2012**, *48*, 6487–6489. [CrossRef] [PubMed]

146. Panzone, C.; Philippe, R.; Chappaz, A.; Fongarland, P.; Bengaouer, A. Power-to-Liquid catalytic CO_2 valorization into fuels and chemicals: Focus on the Fischer-Tropsch route. *J. CO_2 Util.* **2020**, *38*, 314–347. [CrossRef]

147. Jiang, Y.; Chen, F.; Xia, C. A review on cathode processes and materials for electro-reduction of carbon dioxide in solid oxide electrolysis cells. *J. Power Sources* **2021**, *493*, 229713. [CrossRef]

148. Subramanian, K.; Asokan, K.; Jeevarathinam, D.; Chandrasekaran, M. Electrochemical membrane reactor for the reduction of carbondioxide to formate. *J. Appl. Electrochem.* **2007**, *37*, 255–260. [CrossRef]

149. Narayanan, S.; Haines, B.; Soler, J.; Valdez, T. Electrochemical conversion of carbon dioxide to formate in alkaline polymer electrolyte membrane cells. *J. Electrochem. Soc.* **2010**, *158*, A167. [CrossRef]

150. Ampelli, C.; Centi, G.; Passalacqua, R.; Perathoner, S. Synthesis of solar fuels by a novel photoelectrocatalytic approach. *Energy Environ. Sci.* **2010**, *3*, 292–301. [CrossRef]

151. Whipple, D.T.; Finke, E.C.; Kenis, P.J. Microfluidic reactor for the electrochemical reduction of carbon dioxide: The effect of pH. *Electrochem. Solid-State Lett.* **2010**, *13*, B109. [CrossRef]

152. Jayashree, R.S.; Mitchell, M.; Natarajan, D.; Markoski, L.J.; Kenis, P.J. Microfluidic hydrogen fuel cell with a liquid electrolyte. *Langmuir* **2007**, *23*, 6871–6874. [CrossRef] [PubMed]

153. Hatsukade, T.; Kuhl, K.P.; Cave, E.R.; Abram, D.N.; Jaramillo, T.F. Insights into the electrocatalytic reduction of CO_2 on metallic silver surfaces. *Phys. Chem. Chem. Phys.* **2014**, *16*, 13814–13819. [CrossRef] [PubMed]